

Tutorial: 3D toroidal physics - testing the boundaries of symmetry breaking

Don Spong

Oak Ridge National Laboratory

56th Annual Meeting

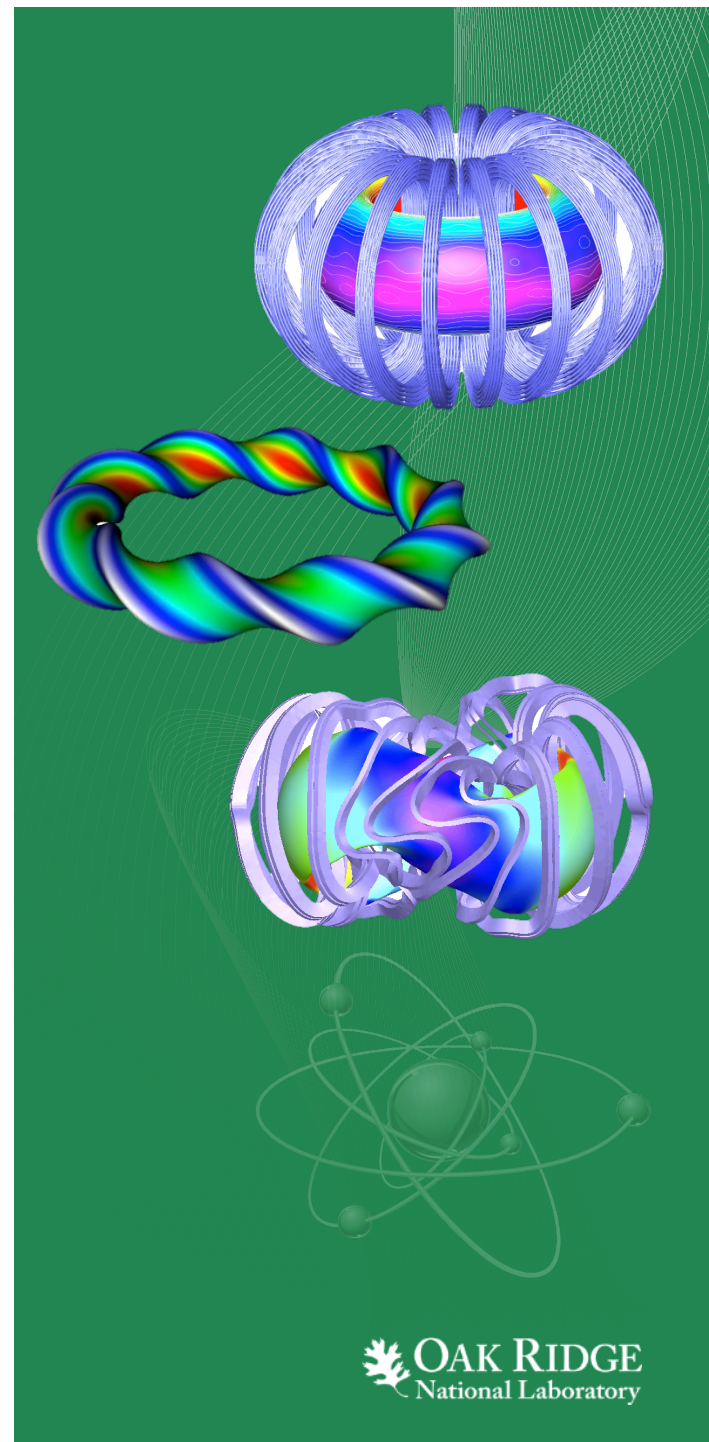
APS Division of Plasma Physics

October 27-31, 2014

New Orleans, Louisiana

Acknowledgements: S. Hirshman, J. Harris, A. Bortolon, D. del-Castillo-Negrete, J. Canik, J. Lore, A. Wingen, A. Briesemeister, H. Weitzner, A. Ware, F. Volpe, A. Cooper, E. Lazarus, A. Boozer, H. Mynick, S. Lazerson, I. Holod, Z. Lin, P. Helander, M. Landremann, A. Turnbull, A. Reimann

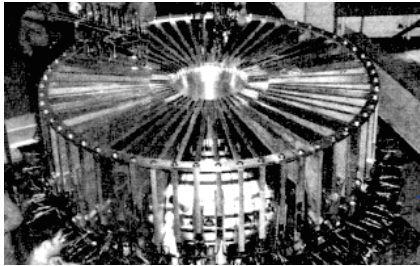
ORNL is managed by UT-Battelle
for the US Department of Energy



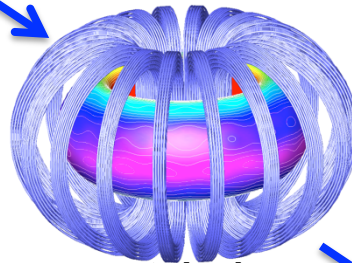
3D symmetry-breaking effects are present in all toroidal fusion configurations

- **Engineering/economic constraints**
 - Finite number of TF coils, ferrous steel structures (blankets, beams, etc.), error fields from fabrication tolerances
 - Particle/energy sources not symmetrically distributed (pellets, beams, RF)
- **Plasma generated**
 - Evolution to lower energy state: macro scale 3D instability structures
 - Single-helicity states in reversed field pinches (RFP)
 - Halo currents, pellet ablation clouds, neutrals, edge plasma blobs
- **Plasma control**
 - Coils for edge localized instabilities, resistive wall instabilities
- **Plasma optimization**
 - Vacuum rotational transform, confinement/stability optimization

The progression of 3D/symmetry-breaking in fusion: tokamaks, mirrors

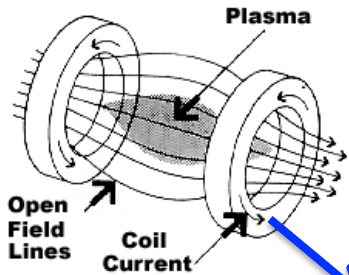


ORMAK (56 TF coils)

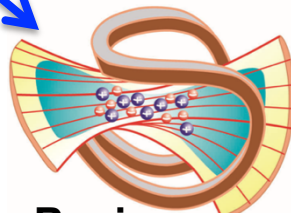


current devices
18-22 TF coils
up-down asymmetry

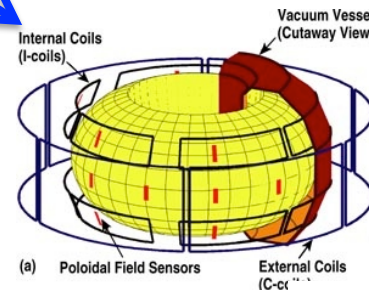
- Tokamaks initially 3D only from
 - Finite number of toroidal coils
 - Conducting shell breaks, field errors
- More recently
 - Fewer TF coils
 - ELM/RWM stability control coils
 - Non-uniform ferritic steel (test-blanket modules)
- Mirror: symmetric, except for field errors
 - Symmetry breaking added (min B) for interchange stability



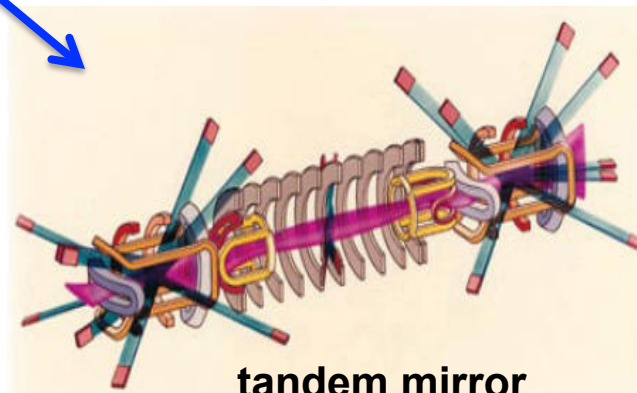
simple mirror



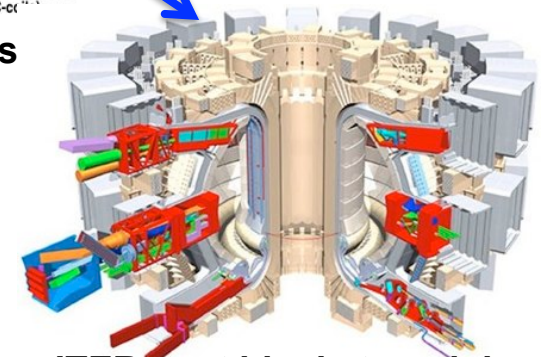
min B mirror



ELM/RWM coils



tandem mirror



ITER: test blanket modules

The progression of 3D/symmetry-breaking in fusion: stellarators, reversed field pinch

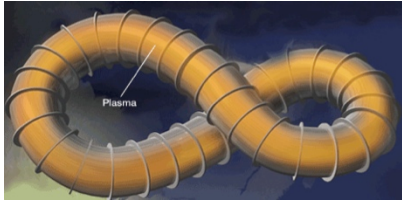
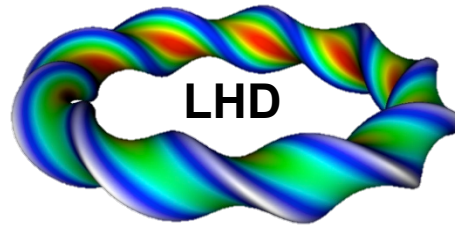


figure-8 stellarator



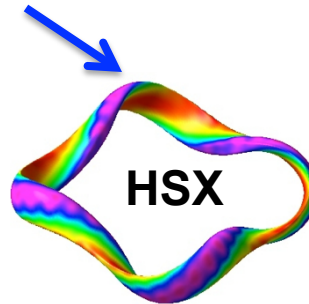
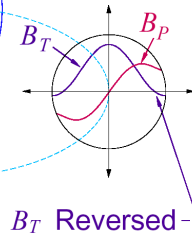
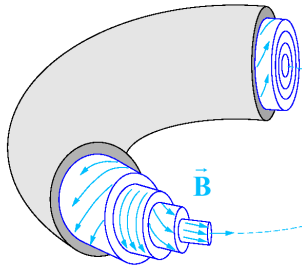
LHD

- Stellarators strongly 3D by design
- Areas of past/ongoing improvement
 - Avoidance of resonant field errors
 - Island suppression: shear, \neq low order n/m
 - Confinement optimization
- Reversed field pinches – spontaneous helical states

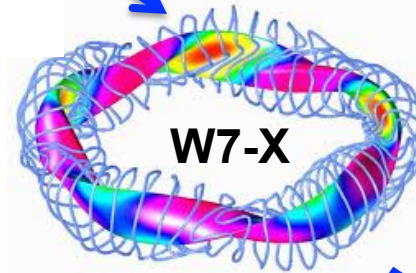


ATF

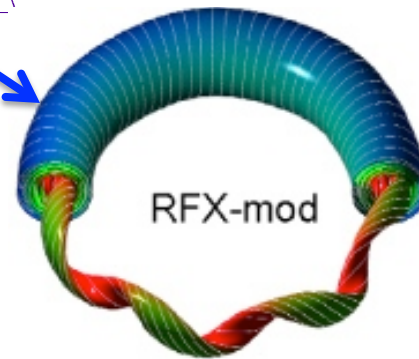
MST, RFX



HSX

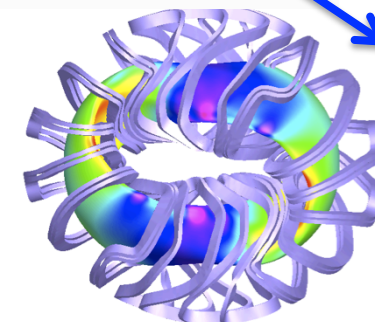


W7-X

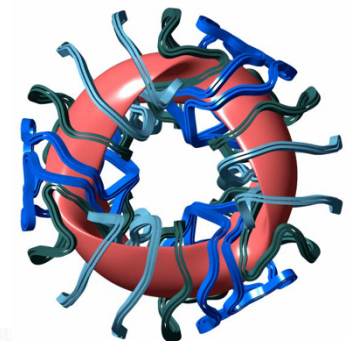


RFX-mod

Self-organized helical state



QPS



NCSX

Symmetry-breaking effects likely to remain and lead to new physics issues

- **Reactors**

- Coils further from plasma, but ports/non-uniformity likely in surrounding ferritic steel structures
- 3D coils for control, rotational transform, optimization → low re-circulating power

- **How much symmetry-breaking can be tolerated?**

- Up to some level masked by turbulence, collisions, ambipolar E_r field, island suppression by flows, etc.
- Lower collisionality regimes of reactors => effects in current experiments may not be reactor compatible
 - Sufficient confinement to maintain H-mode pedestal profiles
 - Neoclassical toroidal viscosity – rotation effects
- Energetic particle confinement, localized wall heat fluxes, lowered ignition margin

- **Advances in 3D simulation tools and diagnostics essential**

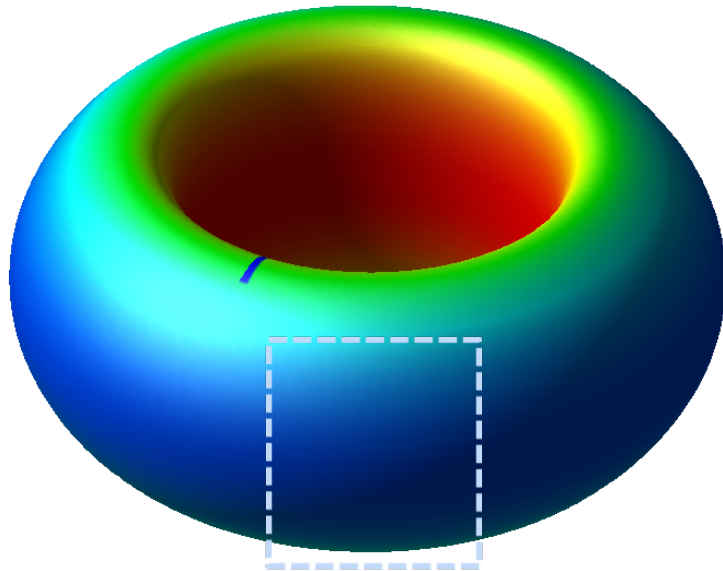
Outline

- **Characteristic forms of symmetry for 3D systems**
 - Field period symmetry, stellarator symmetry
 - Quasi-symmetry in magnetic coordinates (Hamada, Boozer)
 - Approximate degrees of deviation from axisymmetry
 - **3D tokamak** ($\delta B_{n \neq 0} / \delta B_{n=0} = 10^{-3}$ to 10^{-2})
 - **Helical reversed field pinch state** ($\delta B_{n \neq 0} / \delta B_{n=0} = 0.03$ to 0.05)
 - **Stellarator** ($\delta B_{n \neq 0} / \delta B_{n=0} = 0.1$ to 0.3)
 - Resonant ($\delta B_{\perp} \neq 0, m = nq$) vs. non-resonant ($\delta B_{\perp} \sim 0, m \neq nq$)
- **3D design**
- **Equilibrium**
- **Confinement, transport**
- **Stability**
- Many new 3D theory/modeling approaches under development, cannot cover all in this talk

Basic symmetries for 3D systems:

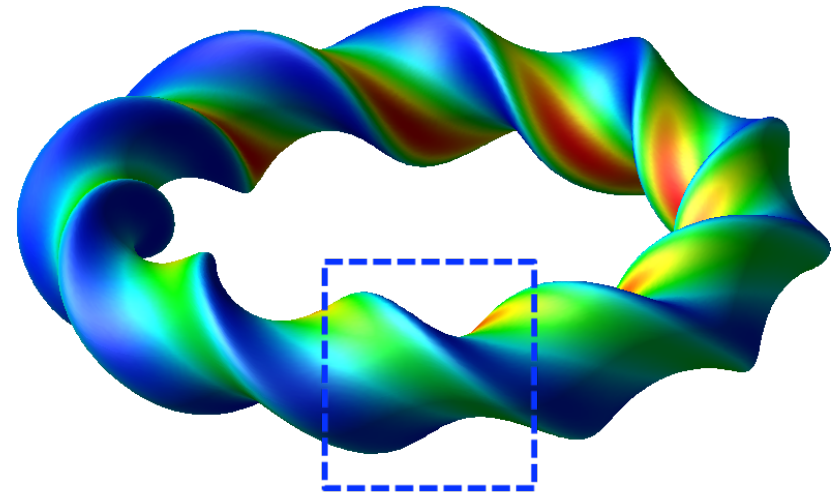
Continuous symmetry:

same view after arbitrary rotation ($N_{fp} \rightarrow \infty$)
 magnetic field is integrable – Hamiltonian
 with an ignorable coordinate



Field period symmetry:

equivalent view after a
 discrete $2\pi/N_{fp}$ rotation
 e.g. = 36° for LHD ($N_{fp} = 10$)



Stellarator symmetry:

Turn around and stand on your
 head for an equivalent view

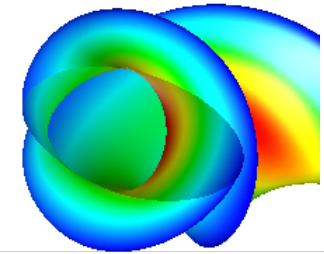
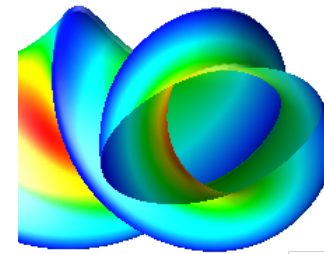
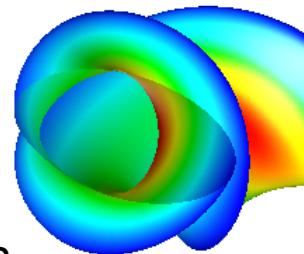
Simplifies analysis:

$R, B \sim \cos(m\theta - n\zeta)$ [~~$\sin(m\theta - n\zeta)$~~]
 maintained in stellarators, but

broken in up-down asymmetric tokamaks

Turn around

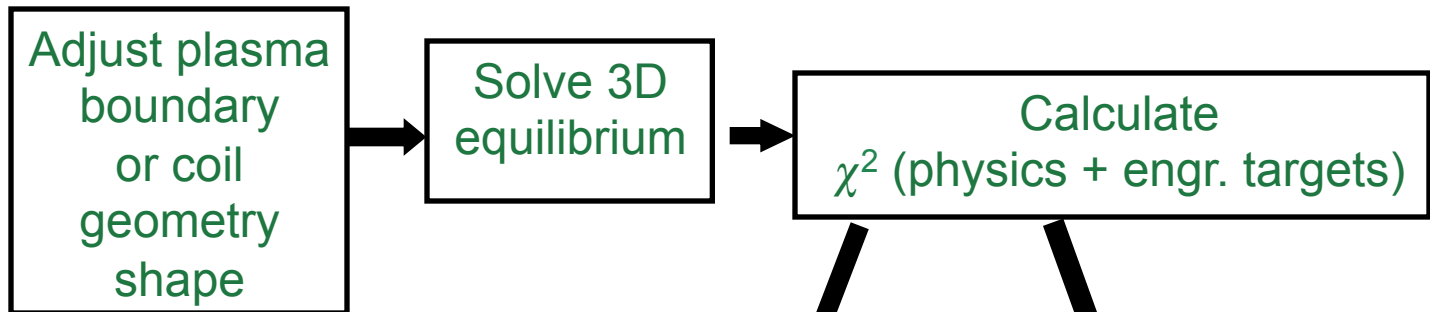
Turn around
 +vertical inversion



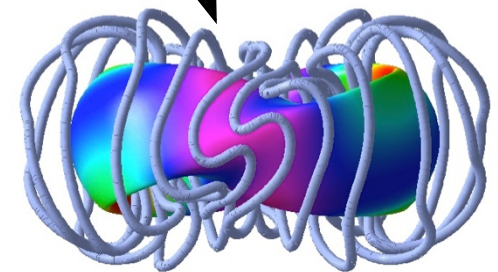
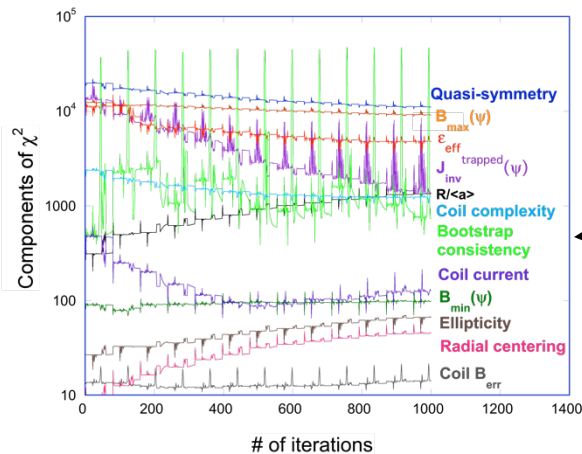
Synthesis of 3D configurations

- Coils \rightarrow outer magnetic surface shape \rightarrow physics properties
- 3D shapes open up very large design space: ~ 40 independent parameters (A. Boozer, L. P Ku, 2010) based on SVD analysis
- Axisymmetric tokamak shape parameters: $\varepsilon, \kappa, \delta$
- Thought experiment: quantize shape parameters into 10 levels
 - 10^3 2D configurations vs. 10^{40} 3D configurations \Rightarrow “combinatorial explosion”
 - Other large numbers: 7×10^{22} visible stars, 6×10^{30} prokaryotes (bacteria) on earth’s surface

• STELLOPT:



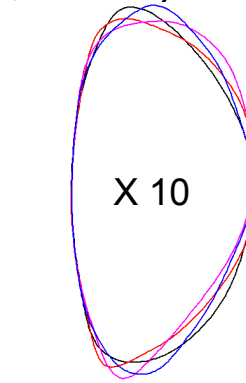
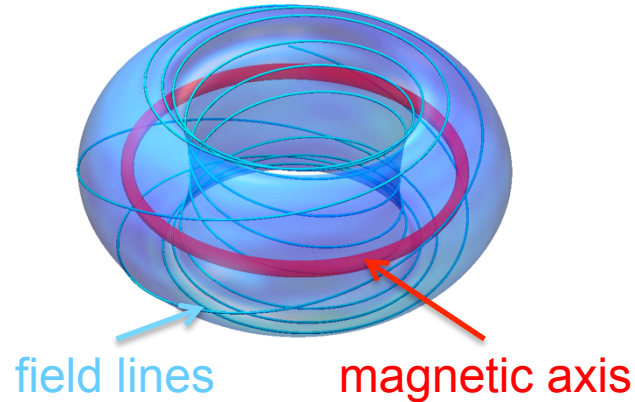
Levenberg-Marquardt
or other method used
to minimize χ^2



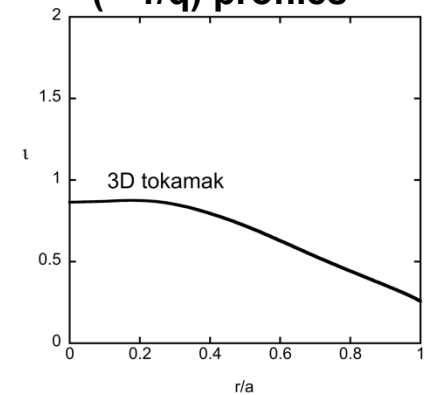
3 methods for creating rotational transform

(L. Spitzer, 1951; C. Mercier, 1964)

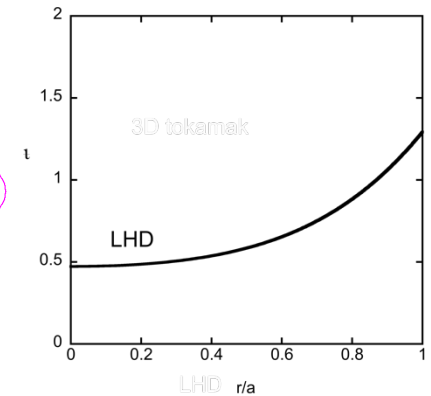
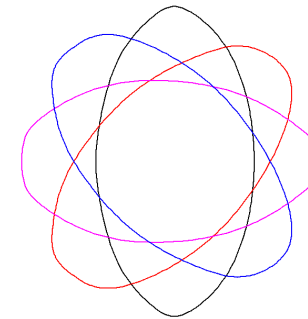
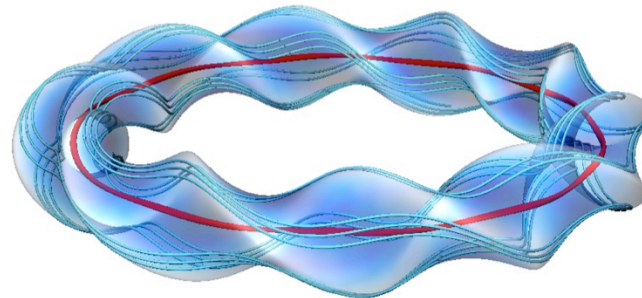
- Plasma current (3D tokamak)



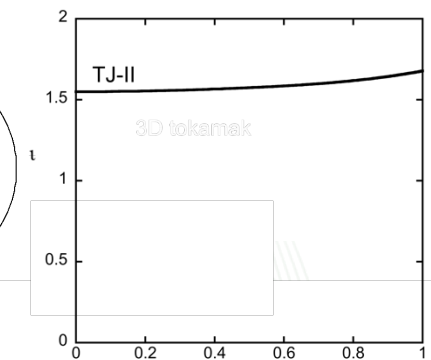
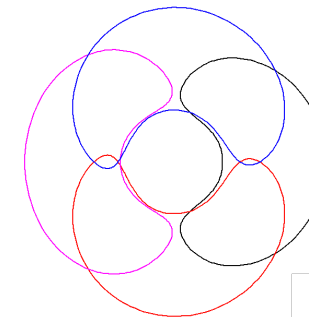
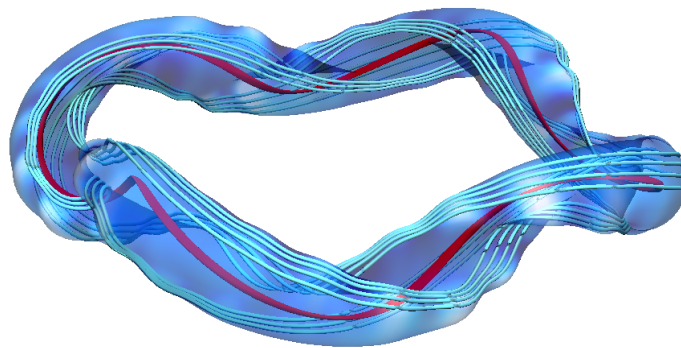
Rotational transform (= 1/q) profiles



- Planar axis, rotating cross-section (LHD, ATF)



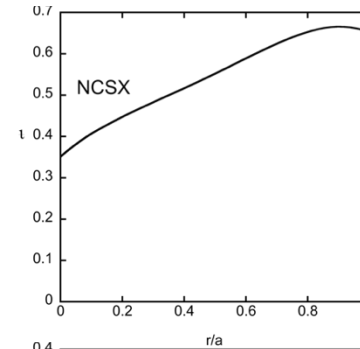
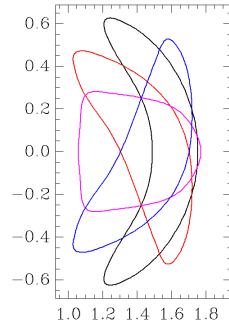
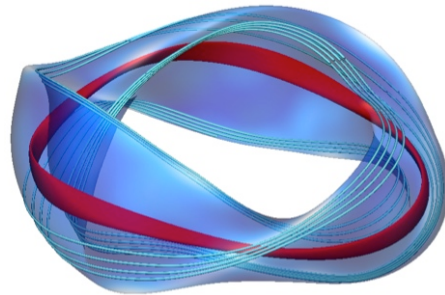
- Helical magnetic axis (TJ-II, HSX, W7-X, H1-NF)



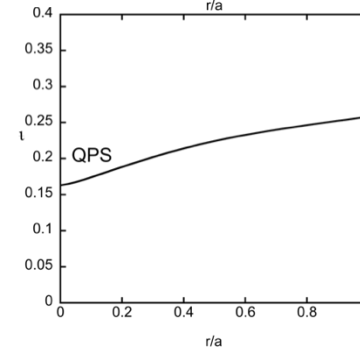
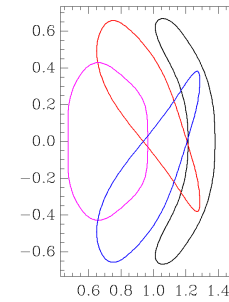
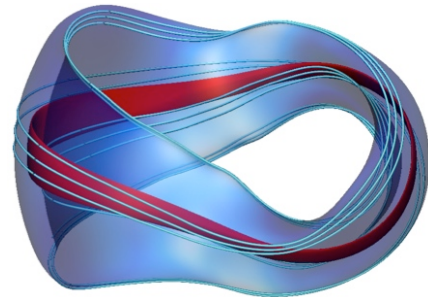
Configuration scaling: $\pm / N_{fp} = \text{const.}$, $\langle R \rangle / \langle a \rangle / N_{fp} = \text{const.}$, $N_{fp} = \text{field periods}$

• Stellarator/tokamak hybrids

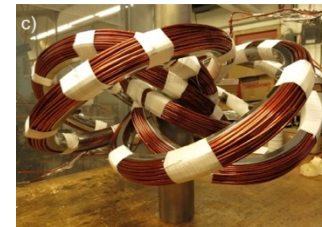
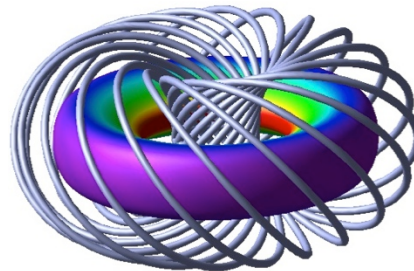
– NCSX



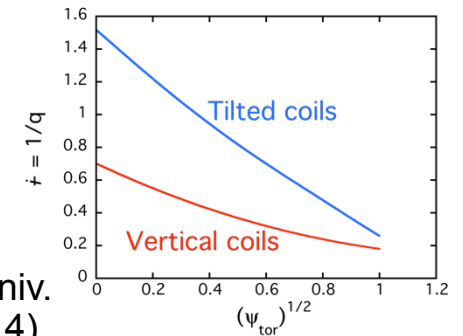
– QPS



– Tilted coils transform amplifier



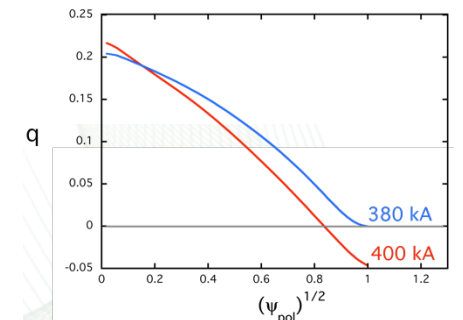
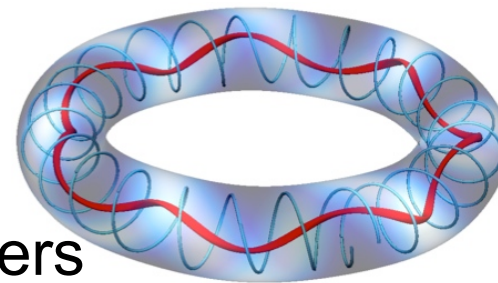
Proto-CIRCUS - Columbia Univ.
A. Clark, F. Volpe, et al. (2014)



• Reverse field pinches

– single helicity states

– sustainment, transport barriers

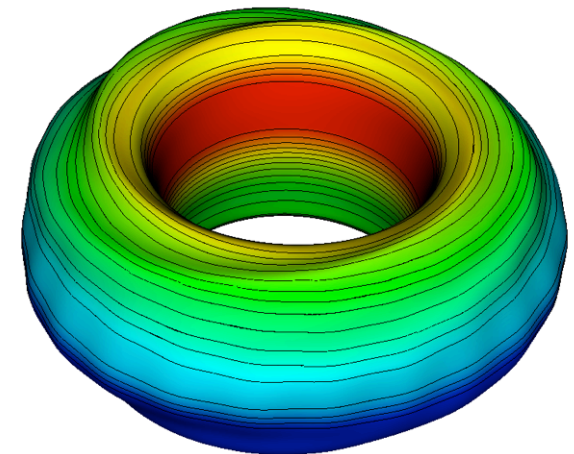


3D tokamaks: ELM/RWM controls

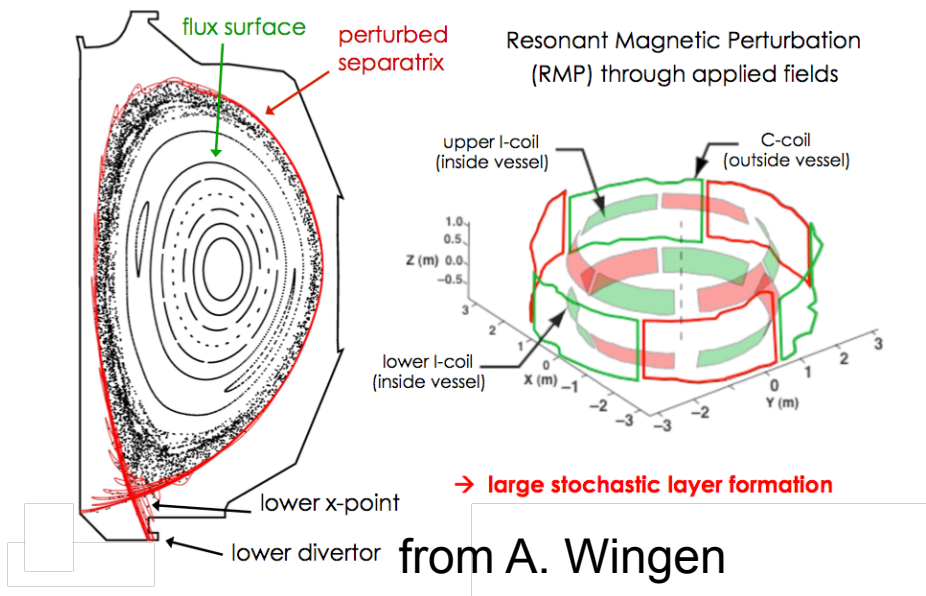
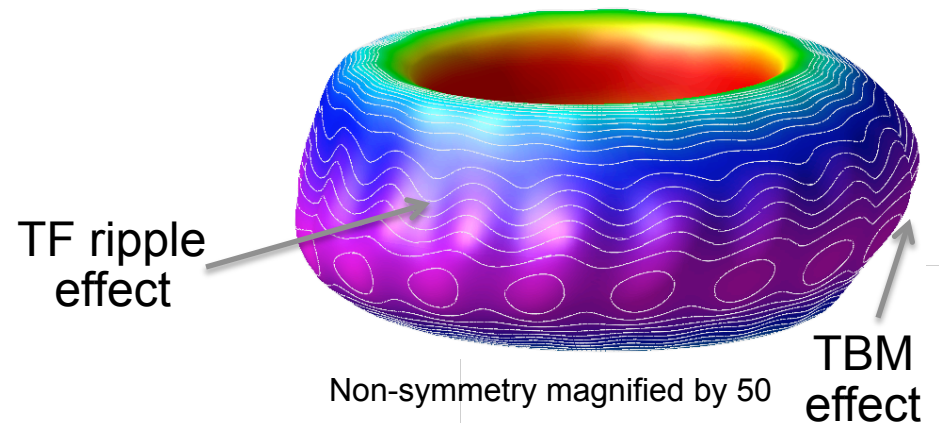
- Window-pane coils → produce magnetic field \perp to outer flux surfaces ($\sim 10^{-3}$ of axisymmetric field)
 - Resonant ($m = nq$) and non-resonant ($m \neq nq$) fields present
 - Goal is to locally break up outer flux surfaces
 - Islands to limit pedestal region
 - suppress edge-localized mode (ELM) instabilities

- TF ripple, test blanket modules, non-symmetric ferritic steel

Resonant fields - ELM coil



Non-resonant fields – TF ripple/TBM



The 3D toroidal equilibrium challenge

- Basic equations

- force balance $\vec{F} = \vec{\nabla}p - \vec{J} \times \vec{B} = 0$

- Ampere's law $\mu_0 \vec{J} = \vec{\nabla} \times \vec{B} \Rightarrow \vec{\nabla} \cdot \vec{J} = 0 \rightarrow W = \int \left(\frac{|\vec{B}|^2}{2\mu_0} + \frac{p}{\gamma - 1} \right) d^3x$

- absence of monopoles $\vec{\nabla} \cdot \vec{B} = 0$

Variational principle
(Kruskal, Kulsrud, 1958)

- Fundamental issues

- Non-existence of 3D nested surface equilibria (Grad, 1967; Lortz, 1971) except for closed field line systems

- Axisymmetry \rightarrow Grad-Shafranov equation (nonlinear elliptic PDE)

- 3D \rightarrow mixed nonlinear hyperbolic/elliptic system (also occurs in transonic flow, lower hybrid wave propagation, Weitzner, 2014)

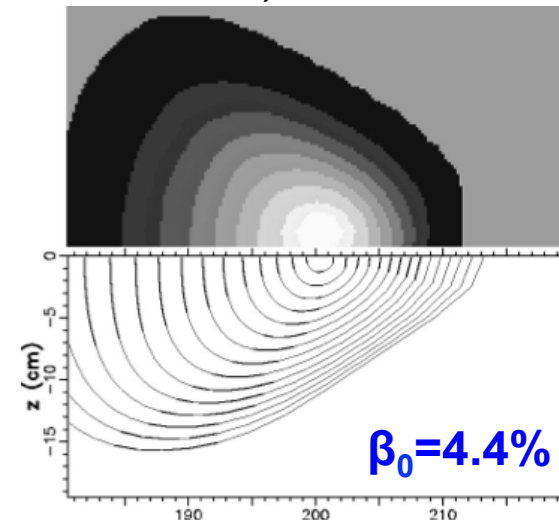
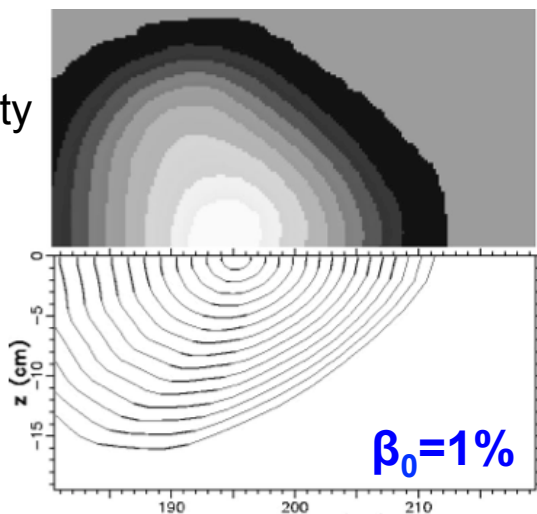
- Singular current sheets at rational surfaces, islands, chaotic field lines

Nested flux surface approach: VMEC (Variational Moments Equilibrium Code)

- **Constrains magnetic field lines to lie on nested flux surfaces** [Hirshman, Whitson (1983)] $\vec{B} = \vec{\nabla}\zeta \times \vec{\nabla}\Phi_{pol} + \vec{\nabla}\theta \times \vec{\nabla}\Phi_{tor}$ $\zeta, \theta =$ toroidal/poloidal angles, $2\pi\Phi_{pol,tor} =$ mag. fluxes
- **Steepest-descent minimization of variational form and force balance**
 - Finds equilibria without fully resolving singular currents
 - generally good approximation to the more exact case with islands
 - Stellarators avoid large islands by magnetic shear or avoiding low order rational i
- **Inverse solution, solves for:** $R = \sum R_{mn}(\Phi_{tor}) \cos(m\theta - n\zeta)$; $Z = \sum Z_{mn}(\Phi_{tor}) \sin(m\theta - n\zeta)$
- **Computationally efficient: used for many 3D physics calculations, stellarator optimization (STELLOPT), 3D reconstruction (V3FIT)**
- **Validation on W7-AS stellarator** (A. Weller, 1999)

X-ray emissivity
contours

Calculated
flux surfaces



3D equilibria with broken flux surfaces

• Nonlinear equilibrium solvers

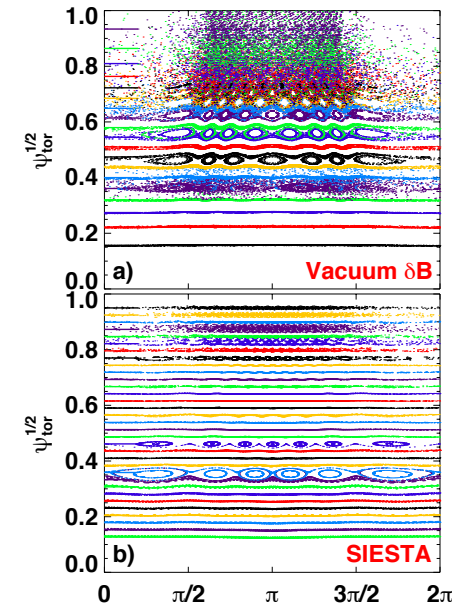
- VMEC \rightarrow SIESTA (direct solver)
 - allows for component of B normal to initial surfaces, also, pressure evolves
- PIES (A. Reiman, 1986), HINT-2 (Y. Suzuki, 2006)
 - direct iterative solvers

• Linearized MHD (takes into account rotation, 2-fluid effects, dissipation)

- Magnetic islands stagnate flows, requires transfer of torque
- M3D-C¹ (N. Ferraro)
- MARS-F (A. Turnbull)
- IPEC (J.-K. Park)

• Other approaches

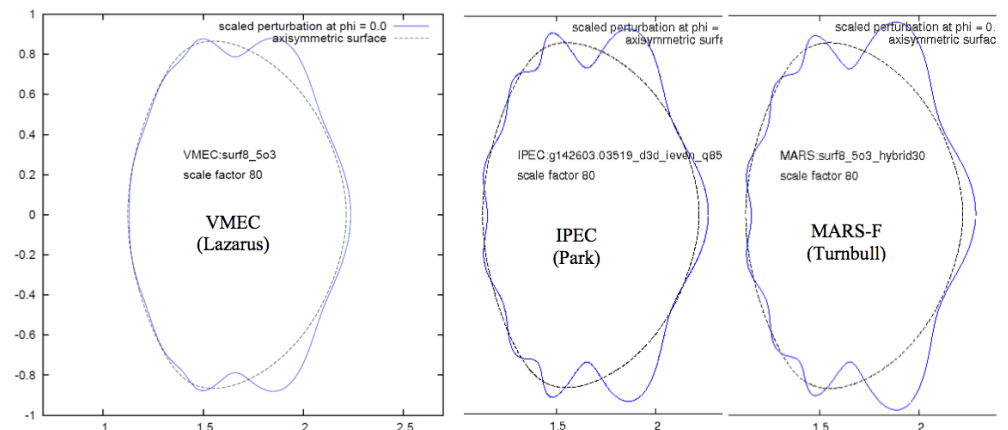
- Discontinuous pressure
 - SPEC (S. Hudson)
 - $dp/dr = 0$ on rational surfaces
- Superposition
 - Vacuum 3D field on 2D equilibrium



NSTX islands with ELM coils
J. Canik (2013)

**$q = 8.5/3$ flux surface comparison
perturbation scaled by factor of 80**

(E. Lazarus, J.-K. Park., A. Turnbull, A. Reiman, 2014)
J. D. King, APS/DPP invited talk T11.04



3D tokamak edge: corrugation, kinks, or peeling/ballooning?

- **New diagnostics**

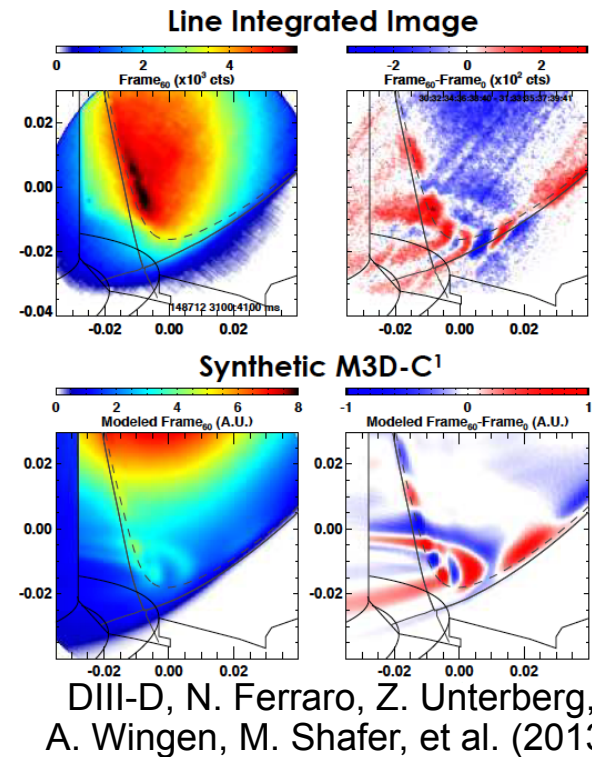
- Soft X-ray emissivity measurement
- Energy filtering → image analysis → reconstruction

- **Transport, stability effects**

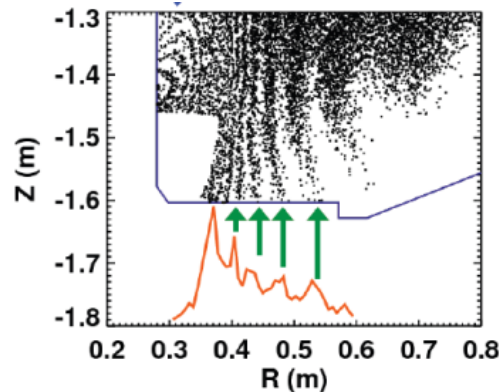
- Rotation braking, density pump-out
- Mode-locking thresholds
- Island screening vs. amplification
- Maintain wall/scrape-off-layer separation

- **Divertor effects**

- Strike point splitting, homoclinic tangles
- Loss of detachment with 3D field application

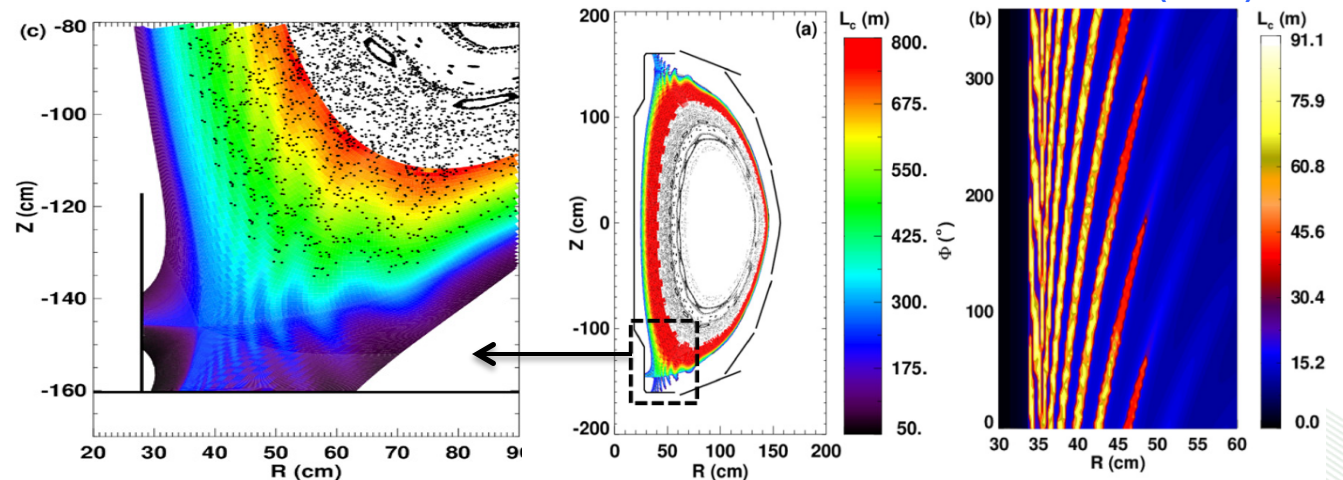


GI1.3 APS/DPP Invited talk (2014)



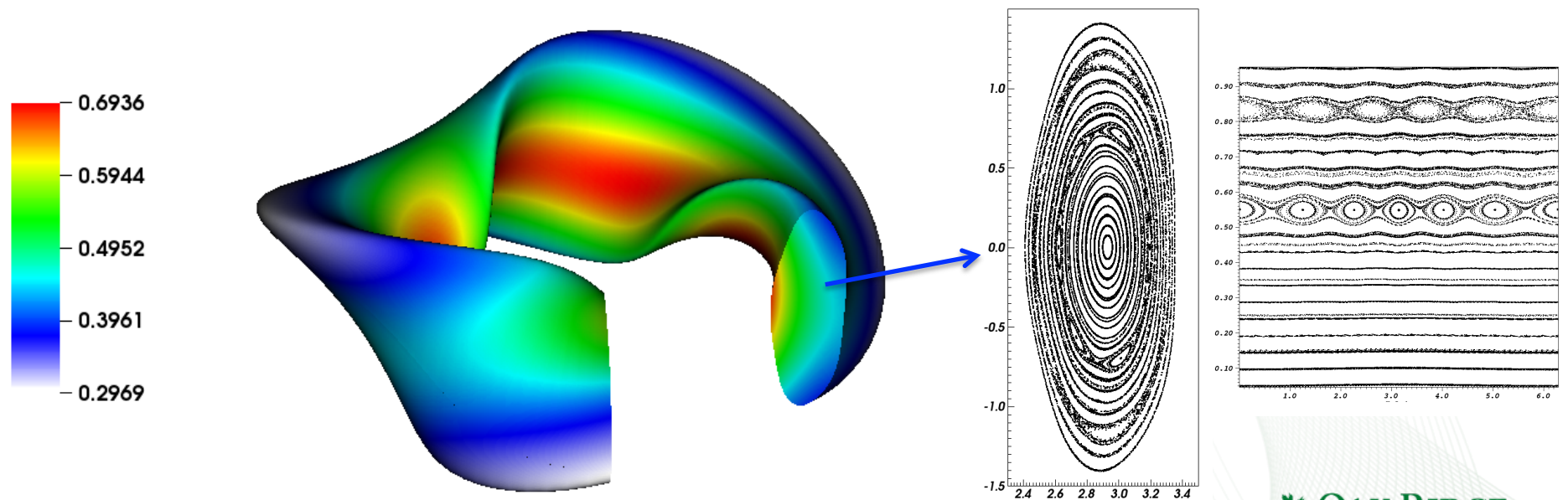
J-W. Ahn, Nucl. Fusion 50, 045010 (2010).

NSTX, J. Lore, EMC3-EIRENE model, TI1.1 APS/DPP Invited talk (2014)



Application of SIESTA to stellarators

- Due to the lack of a continuous symmetry, stellarators have regions with island structures
- **NCSX/QPS** optimization experience showed these islands can be minimized by coil design
- Original motivation for the development of SIESTA: provide a rapidly evaluated target function for **island minimization**
- Also important for physics/transport modeling



Island chain in compact stellarator

Particle Orbits in 3D fields

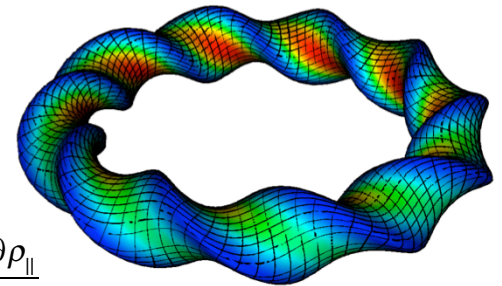
- **Guiding-center**

- Canonical coordinates (A. Boozer, R. White, 1981)

- Only involves $|B|$ and currents in straight field line coordinates

$$\frac{d\psi}{dt} = \frac{1}{D} \left(I \frac{\partial B}{\partial \zeta} - g \frac{\partial B}{\partial \theta} \right) \left(\mu + \frac{mv_{\parallel}^2}{B} \right); \quad \frac{d\rho_{\parallel}}{dt} = \frac{-\rho_{\parallel} g'}{D} \dot{P}_{\theta} + \frac{\rho_{\parallel} l'}{D} \dot{P}_{\zeta}$$

$$\frac{d\theta}{dt} = \left[\left(\mu + \frac{mv_{\parallel}^2}{B} \right) \frac{\partial B}{\partial \psi} + e \frac{\partial \Phi}{\partial \psi} \right] \frac{\partial \psi}{\partial P_{\theta}} + e B v_{\parallel} \frac{\partial \rho_{\parallel}}{\partial P_{\theta}}; \quad \frac{d\zeta}{dt} = \left[\left(\mu + \frac{mv_{\parallel}^2}{B} \right) \frac{\partial B}{\partial \psi} + e \frac{\partial \Phi}{\partial \psi} \right] \frac{\partial \psi}{\partial P_{\zeta}} + e B v_{\parallel} \frac{\partial \rho_{\parallel}}{\partial P_{\zeta}}$$



- Non-canonical coordinates (Littlejohn, Cary 1979-83)

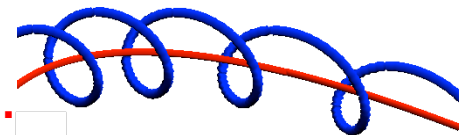
- Lie-transform perturbation methods, variational action integral

- Coordinate-free $\frac{d\vec{R}}{dt} = \frac{1}{B_{\parallel}^*} \left(v_{\parallel} \vec{B}^* + \vec{E}^* \times \hat{b} + \frac{\mu \hat{b} \times \vec{\nabla} B}{Ze} \right); \quad \frac{dv_{\parallel}}{dt} = Ze (\vec{E}^* + \vec{R} \times \vec{B}^*) \cdot \mu \vec{\nabla} B$

$$\vec{B}^* = \vec{B} + \frac{mv_{\parallel}}{Ze} \vec{\nabla} \times \hat{b}; \quad \vec{E}^* = \vec{E} - \frac{mv_{\parallel}}{Ze} \frac{\partial \hat{b}}{\partial t}$$

- **Lorentz equation:** $\frac{d\vec{v}}{dt} = \frac{Ze}{m} (\vec{E} + \vec{v} \times \vec{B})$

G.C.

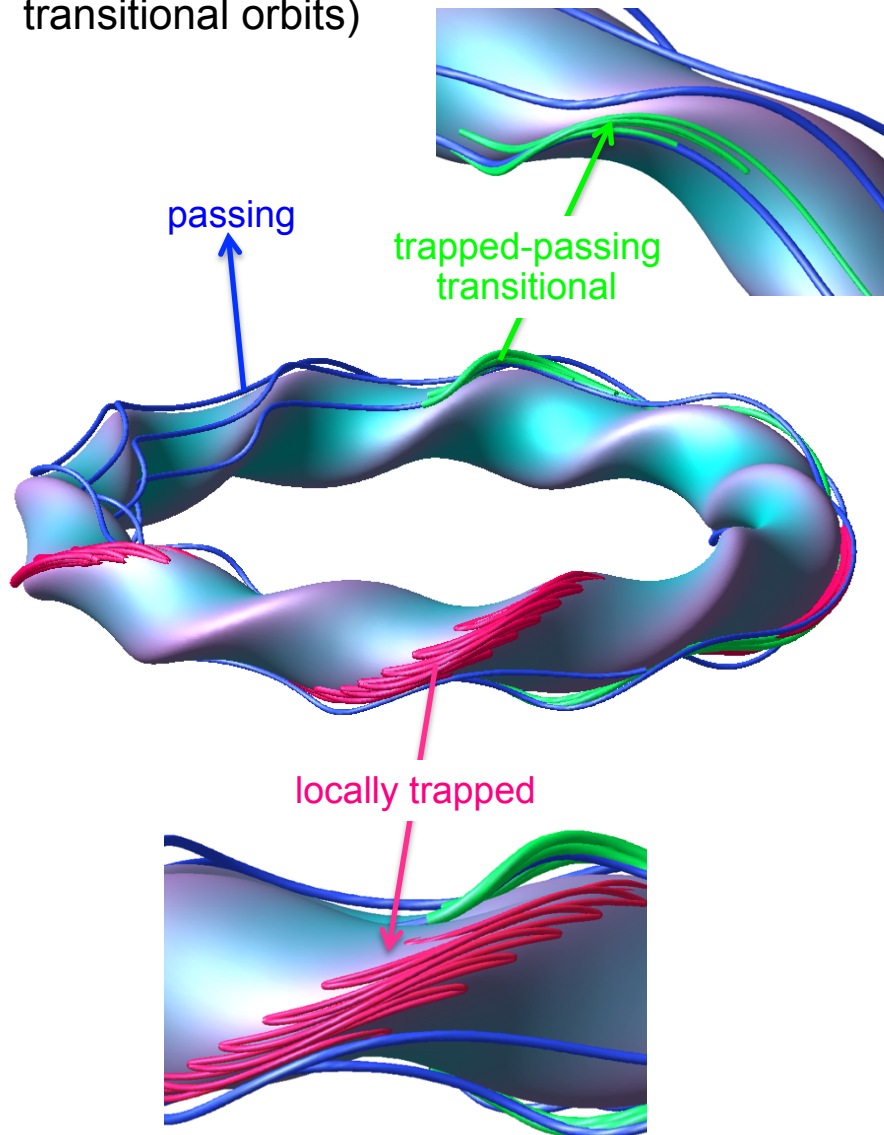


Issues for simulations: energy conservation, Liouville's theorem (conservation of phase space volume carried with particle), intersections of fast ion with walls, PFCs

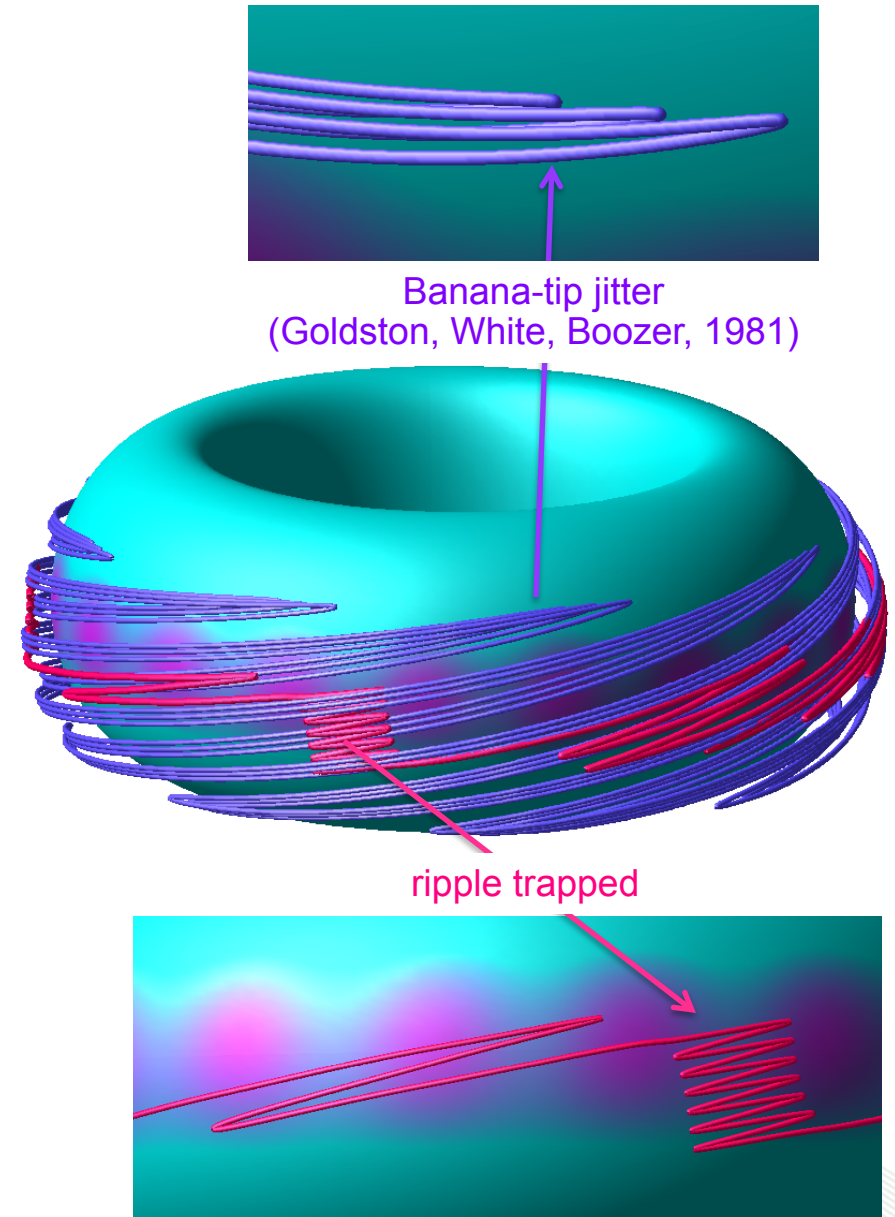
$$\frac{1}{\sqrt{g}} \frac{\partial}{\partial z^i} \left(\sqrt{g} \frac{\partial z^i}{\partial \tau} \right) = 0$$

Particle trajectories in 3D configurations: many new classes of orbits

Stellarator (E_r added for confinement of trapped and transitional orbits)

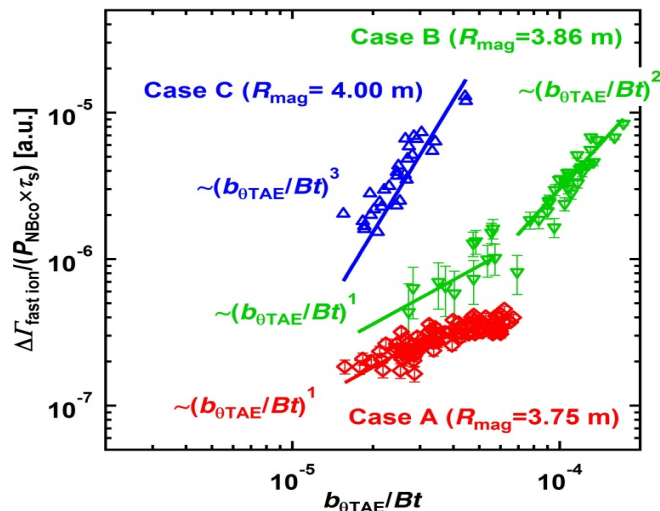
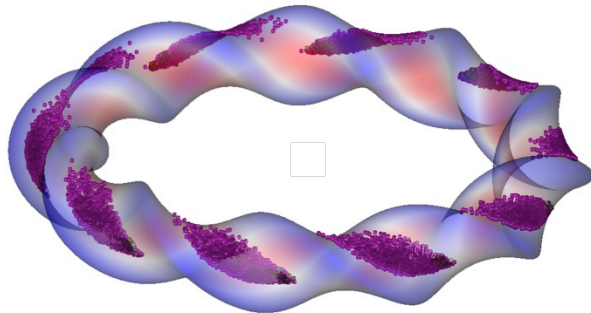


Tokamak with ripple and TBM



Particle Monte Carlo simulations used extensively for energetic particle confinement studies in 3D systems

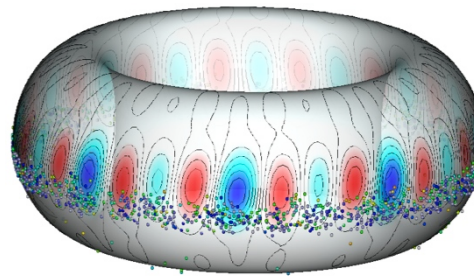
Stellarator neutral beam transport



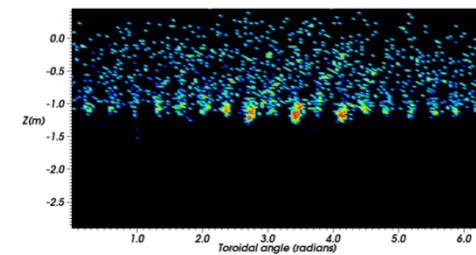
Loss scaling in LHD – K. Ogawa

Tokamaks with 3D perturbations

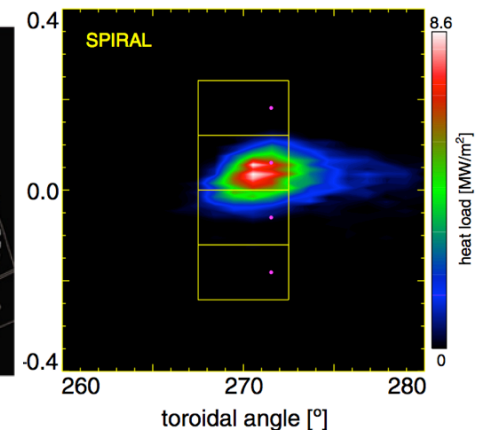
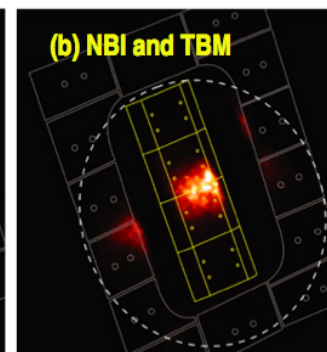
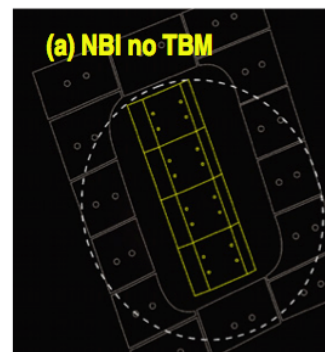
Fast ion exit locations
ITER (TF+TBM)



Wall heat load
localization (D. Spong 2011)



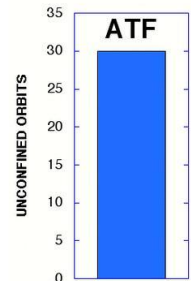
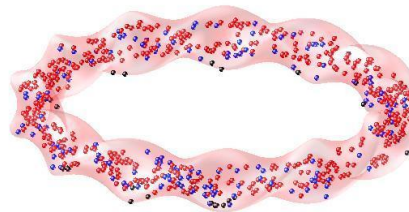
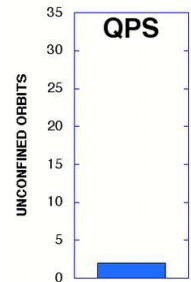
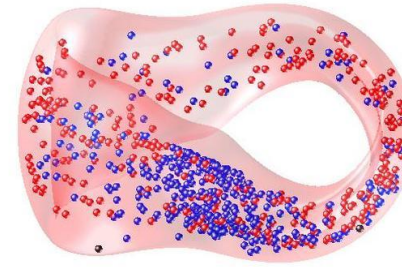
Fast ion losses in DIII-D with TBM
coils (SPIRAL code, G. Kramer, 2011-2013)



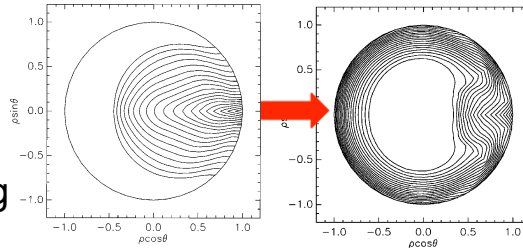
RWM coils: ASCOT and SPIRAL show
EP losses go to divertor plates

Orbit characteristics have also been a dominant factor in stellarator optimization

- Quasi-symmetry $B = B(\psi, M\Theta - N\zeta)$
Nührenberg, Zille (1988)
 - Dual meaning: (1) hidden, (2) approximate
 - Quasi-helical (M,N integers)/toroidal (N=0)/poloidal (M=0)
 - Transport isomorphic to an tokamak



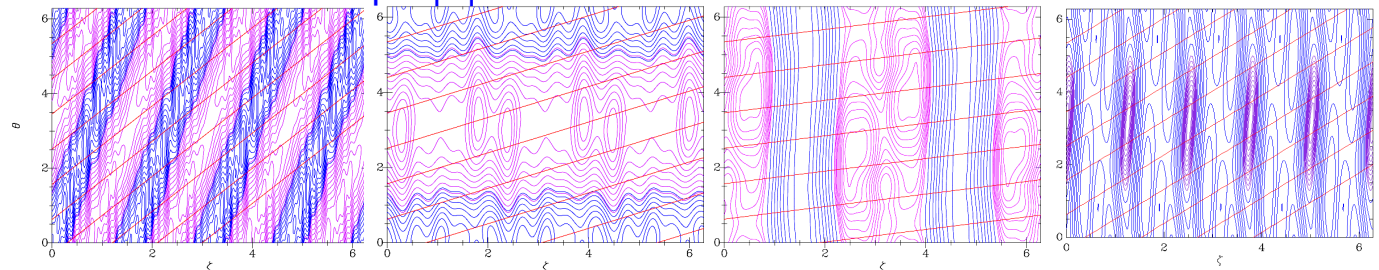
- Quasi-omnigeneity
 - $J = \oint v_{\parallel} dl = J(\psi)$
 - Constant $|B|$ contour spacing



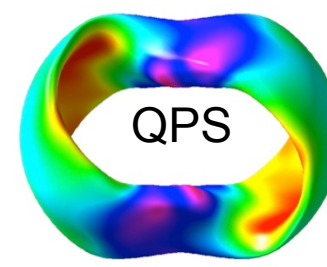
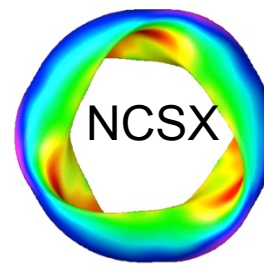
D. Spong, S. Hirshman, et al. (STELLOPT, 1998)

- Quasi-isodynamic
 - Poloidally closed $|B|$ contours

Example $|B|$ contours and field lines in Boozer coordinates

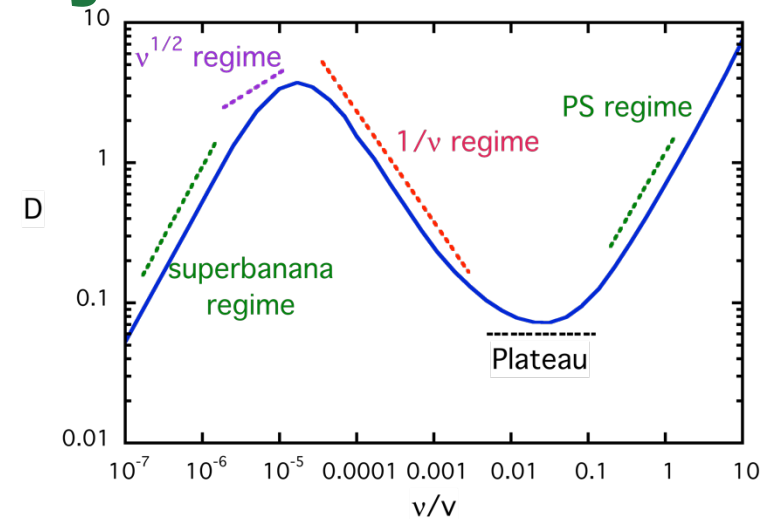


- B_{\min} and B_{\max}
 - Min/max along field line
 - Const. on flux surface
 - Deeply trapped: $B_{\min}(\psi)$
 - Transitional: $B_{\max}(\psi)$



Collisional transport in 3D systems

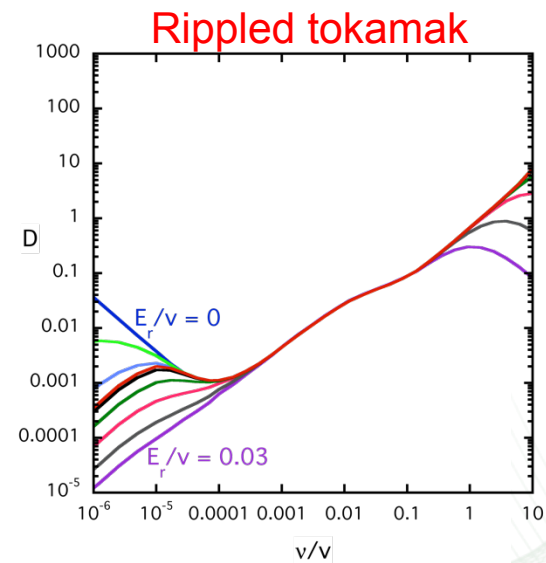
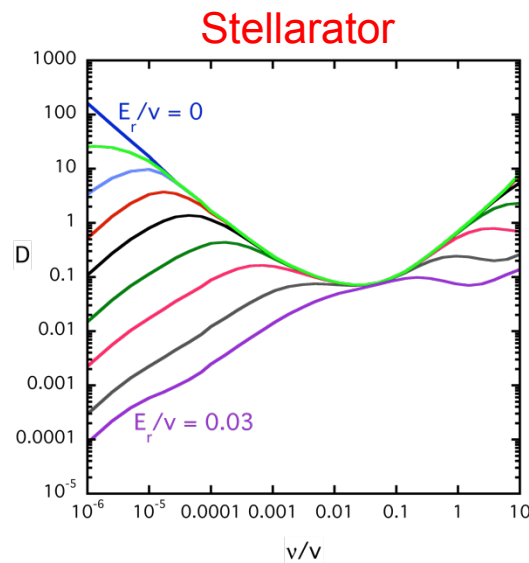
- Characteristics unique to 3D
 - ripple transport regime ($1/\nu$) - trapped particle uncompensated radial drifts
 - ambipolarity condition: $\Gamma_{\text{ion}} = \Gamma_{\text{electron}}$ only for specific E_r
 - Stronger dependence on E_r than tokamak
 - Bootstrap current can be suppressed or reversed
 - Flows in direction of highest symmetry
 - Collisionality and E_r variation – low ripple moves $1/\nu$ to lower collisionality



$$D \propto v_d^2 / \nu \quad \text{Uncompensated radial trapped drifts}$$

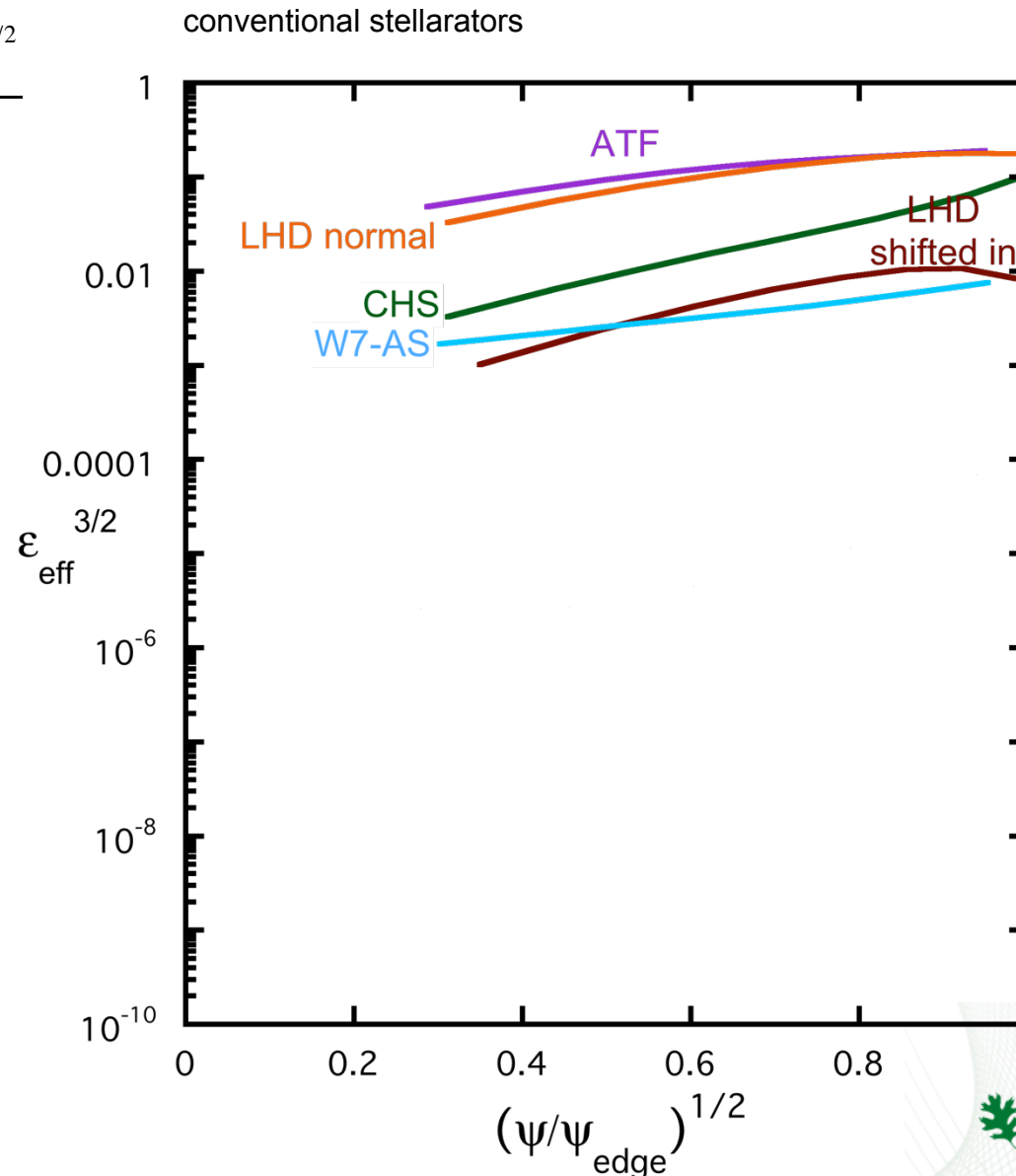
$$D \propto v_d^2 (RB / E_r)^{3/2} \nu^{1/2} \quad \text{Trapping/detrapping from collisions}$$

$$D \propto v_d (v_d RB / E_r)^2 \nu \quad \text{Trapping/detrapping from drifts}$$



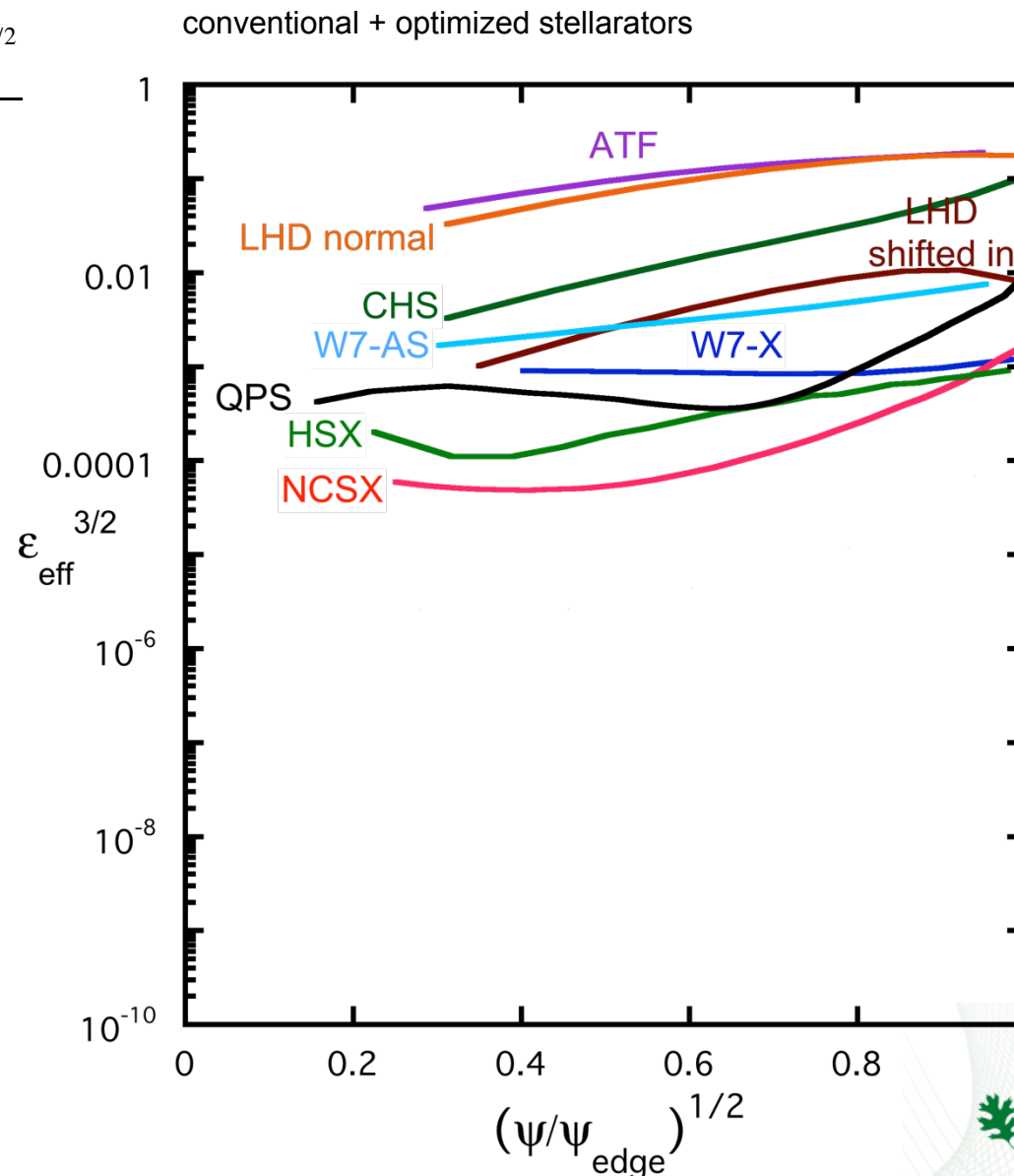
Useful characterization of ripple transport levels: effective ripple parameter

- $D_{1/\nu} / D_{plateau} = \left(\frac{4}{3\pi} \right)^2 \frac{(2\varepsilon_{eff})^{3/2}}{\nu^*}$
- Nemov, Kasilov, Kernbichler (1999)
- $\varepsilon_{eff} = 0$ for ideal tokamak, quasi-symmetry, or quasi-omnigeneity
- Simple measure of orbit deviations from ideal



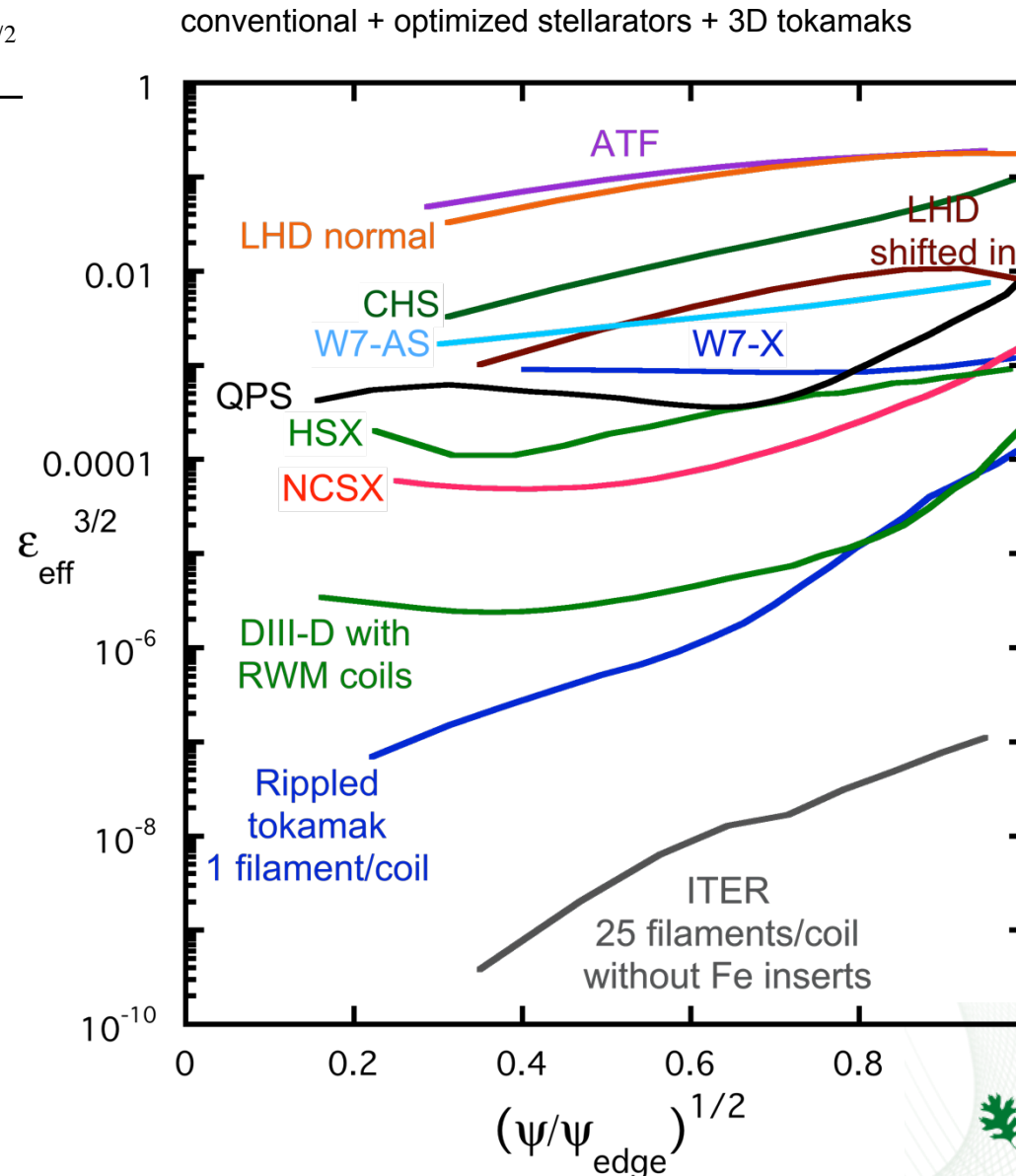
Useful characterization of ripple transport levels: effective ripple parameter

- $D_{1/v} / D_{plateau} = \left(\frac{4}{3\pi} \right)^2 \frac{(2\varepsilon_{eff})^{3/2}}{v^*}$
- Nemov, Kasilov, Kernbichler (1999)
- $\varepsilon_{eff} = 0$ for ideal tokamak, quasi-symmetry, or quasi-omnigeneity
- Simple measure of orbit deviations from ideal



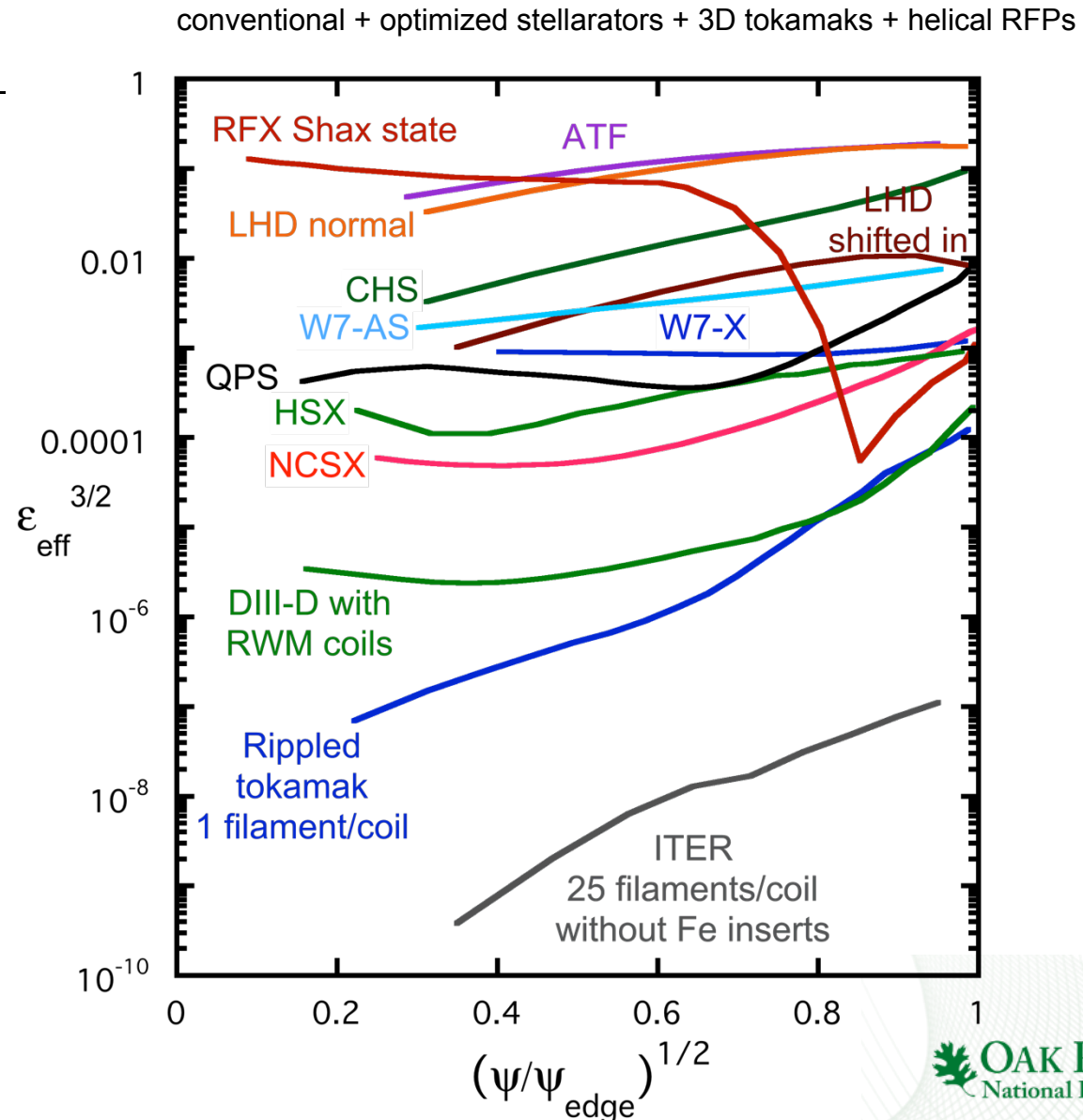
Useful characterization of ripple transport levels: effective ripple parameter

- $D_{1/v} / D_{plateau} = \left(\frac{4}{3\pi} \right)^2 \frac{(2\varepsilon_{eff})^{3/2}}{v^*}$
- Nemov, Kasilov, Kernbichler (1999)
- $\varepsilon_{eff} = 0$ for ideal tokamak, quasi-symmetry, or quasi-omnigeneity
- Simple measure of orbit deviations from ideal



Useful characterization of ripple transport levels: effective ripple parameter

- $D / D_{plateau} = \left(\frac{4}{3\pi} \right)^2 \frac{(2\varepsilon_{eff})^{3/2}}{v^*}$
- Nemov, Kasilov, Kernbichler (1999)
- $\varepsilon_{eff} = 0$ for ideal tokamak, quasi-symmetry, or quasi-omnigeneity
- Simple measure of orbit deviations from ideal



Transport coefficient calculations in 3D systems

- Drift Kinetic Equation Solver (DKES) W. van Rij, S. Hirshman (1989)

- 3D: toroidal/poloidal angle, v_{\parallel}/v – energy and radius, parameters, pitch angle scattering only,
incompressible E x B approximation: $\vec{E} \times \vec{B} / B^2 \approx \vec{E} \times \vec{B} / \langle B^2 \rangle$

- Ripple-averaged GSRAKE (C. Beidler, et al., 1995)

- δf Monte Carlo (MOCA, VENUS, FORTEC-3D) – verification study (C. Beidler, et al., NF, 2011)

- Moments method: correction for momentum non-conservation in DKES coefficients (H. Sugama, S. Nishimura, 2002; M. Taguchi, 1992)

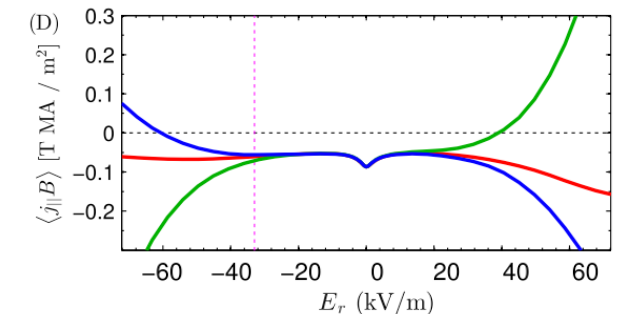
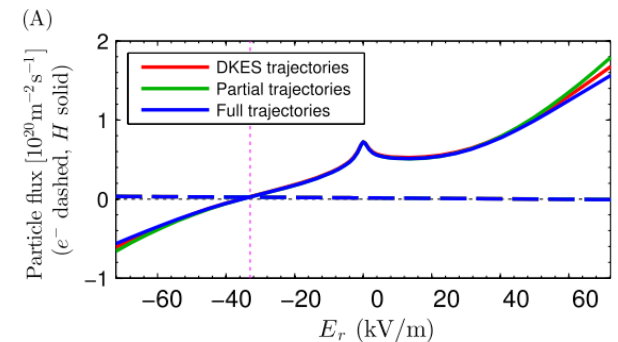
- 4D (toroidal/poloidal angle, v_{\parallel}/v , energy SFINCS) M. Landremann (2014)

- Momentum conserving collisions, full drift trajectories, local diffusive in radius

- Impurity transport with $\phi = \phi(\rho, \theta, \zeta)$ (J.M. García-Regaña, 2013; C. Beidler, 1995)

- 3D tokamak NTV (neoclassical toroidal viscosity) J. D. Callen, IAEA-2010, K. Shaing, 2003-10

$\delta B/B < \rho_{\text{ion}}/a$ regime

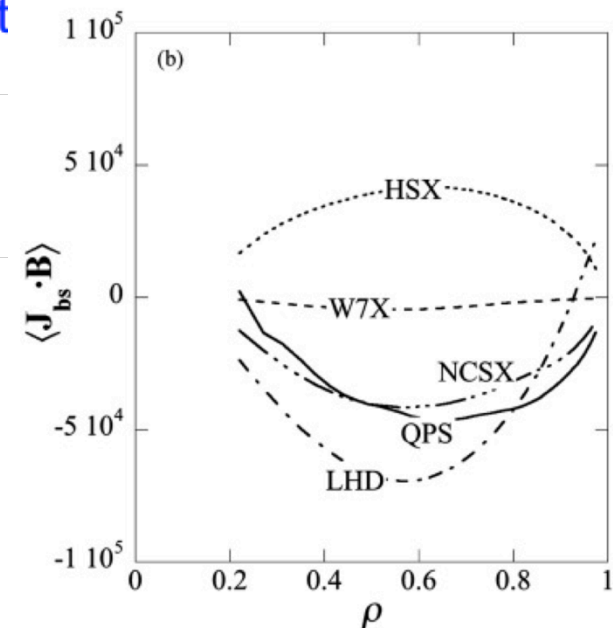


DKES/SFINCS comparisons
for W7-X, M. Landremann (2014)
APS/DPP 2014 Invited talk B11.5

PENTA model – self-consistent (ambipolar) flows, currents with momentum corrections from Sugama, Nishimura method

Radial particle flows required for ambipolar condition \Rightarrow self-consistent energy fluxes and bootstrap current

$$\begin{bmatrix} \Gamma_e \\ q_e / T_e \\ \Gamma_i \\ q_i / T_i \\ J_{BS}^E \end{bmatrix} = \begin{bmatrix} L_{11}^{ee} & L_{12}^{ee} & L_{11}^{ei} & L_{12}^{ei} & L_{1E}^e \\ L_{21}^{ee} & L_{22}^{ee} & L_{21}^{ei} & L_{22}^{ei} & L_{2E}^e \\ L_{11}^{ie} & L_{12}^{ie} & L_{11}^{ii} & L_{12}^{ii} & L_{1E}^i \\ L_{21}^{ie} & L_{22}^{ie} & L_{21}^{ii} & L_{22}^{ii} & L_{2E}^i \\ L_{E1}^e & L_{E2}^e & L_{E1}^i & L_{E2}^i & L_{EE} \end{bmatrix} \begin{bmatrix} X_{e1} \\ X_{e2} \\ X_{i1} \\ X_{i2} \\ X_E \end{bmatrix}$$



A. Ware, FS&T (2006)

Parallel mass and energy flows:

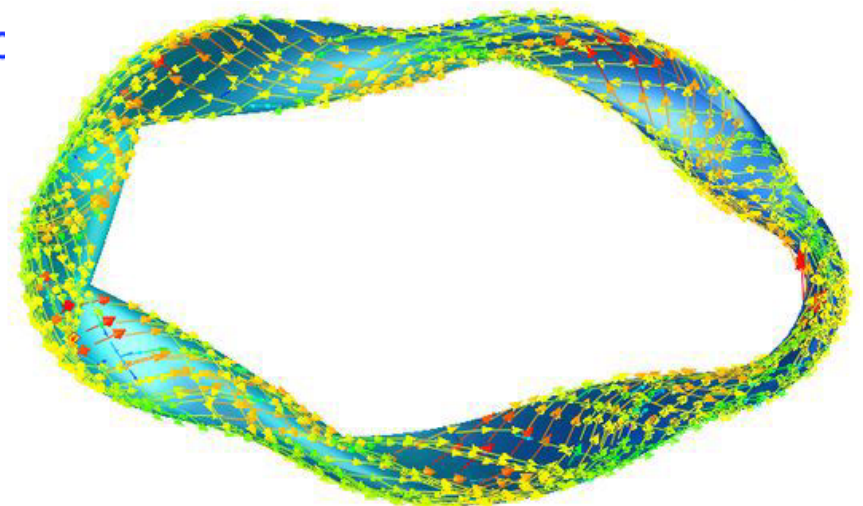
$$\begin{bmatrix} \langle Bu_{\parallel i} \rangle \\ \frac{2}{5p_i} \langle Bq_{\parallel i} \rangle \end{bmatrix} = \left[\frac{1}{\langle B^2 \rangle} \begin{bmatrix} M_{i1} & M_{i2} \\ M_{i2} & M_{i3} \end{bmatrix} - \begin{bmatrix} l_{11}^{ii} & -l_{12}^{ii} \\ -l_{12}^{ii} & l_{22}^{ii} \end{bmatrix} \right]^{-1} \begin{bmatrix} N_{i1} & N_{i2} \\ N_{i2} & N_{i3} \end{bmatrix} \begin{bmatrix} X_{i1} \\ X_{i2} \end{bmatrix}$$

Poloidal and toroidal (contra-variant) flow veloc

$$\begin{bmatrix} \langle u_i^\theta \rangle \\ \langle u_i^\zeta \rangle \end{bmatrix} = \frac{4\pi^2}{V'} \begin{bmatrix} \chi' & -B_\zeta / \langle B^2 \rangle \\ \psi' & B_\theta / \langle B^2 \rangle \end{bmatrix} \begin{bmatrix} \langle Bu_{\parallel i} \rangle / \langle B^2 \rangle \\ X_{i1} \end{bmatrix}$$

$$\text{where } X_{a1} \equiv -\frac{1}{n_a} \frac{\partial p_a}{\partial s} - e_a \frac{\partial \Phi}{\partial s}, \quad X_{a2} \equiv -\frac{\partial T_a}{\partial s}, \quad X_E = \langle BE_{\parallel} \rangle / \langle B^2 \rangle^{1/2}$$

H. Sugama, S. Nishimura, 2002; M. Taguchi, 1992;
D. A. Spong, Phys. Plasmas, 2005



HSX provides test of parallel neoclassical transport properties for quasi-helical symmetry

PENTA code calculates plasma flow over wide range of ripple ϵ_{eff} :
 tokamaks \rightarrow rippled tokamaks \rightarrow quasi-symmetric \rightarrow conventional stellarators

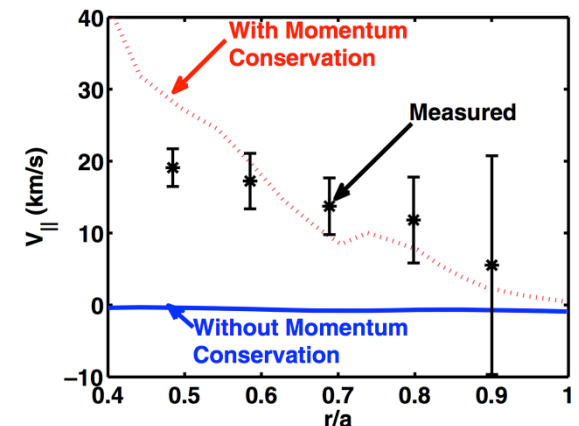
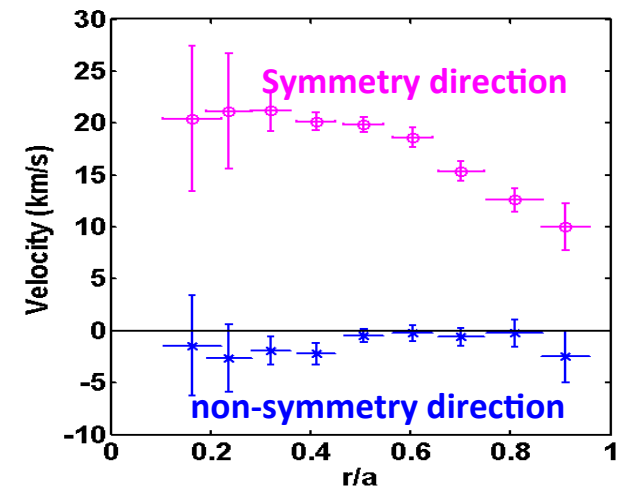
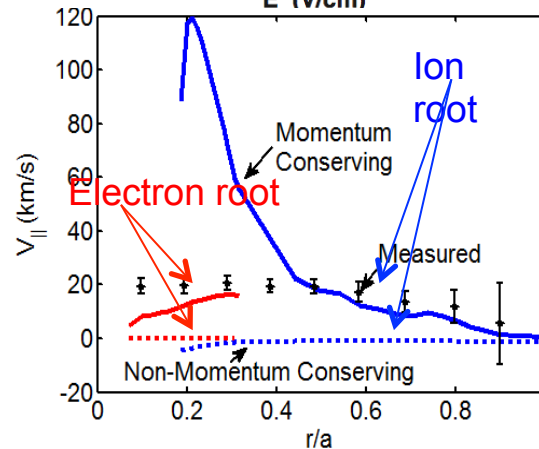
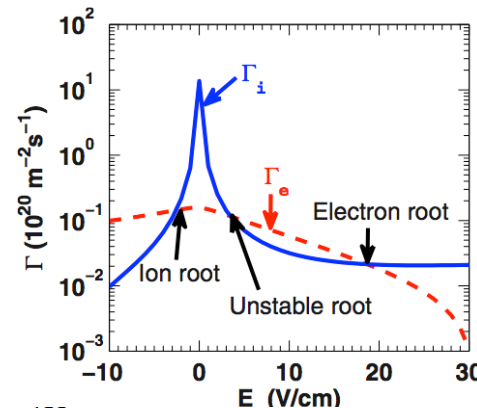
ITER $\sim 10^{-6}$ NSTX w/RMP $\sim 10^{-4}$ HSX $\sim 3 \times 10^{-3}$ LHD, TJ-II $\sim 0.05 - 1$

HSX: CXRS measure large flow in direction of quasi-symmetry

Parallel flows in HSX agree well with PENTA:

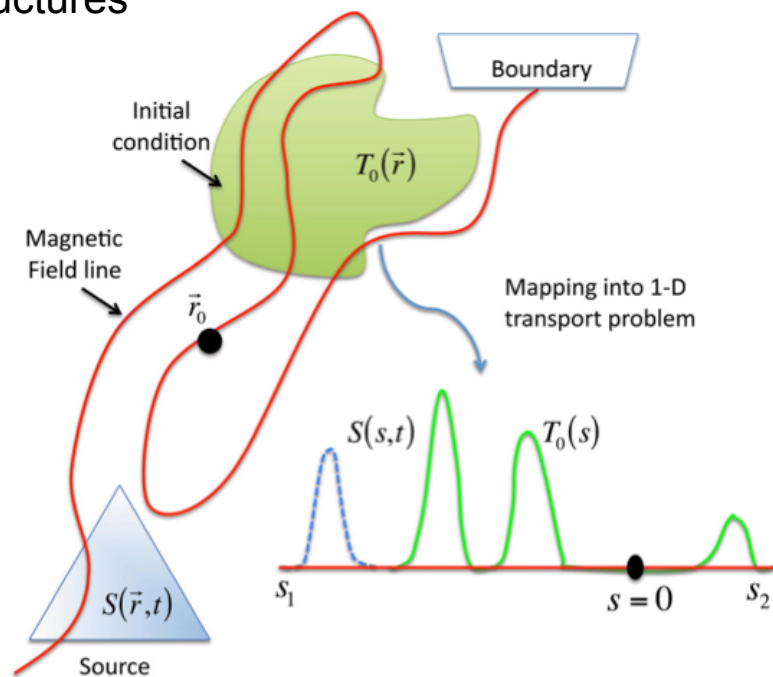
- Importance of momentum conservation
- Large sheared flows reduce turbulent transport

J. Lore, et al., Phys. Plasmas (2010)
 A. Bresemeister, et al., PPCF (2013)

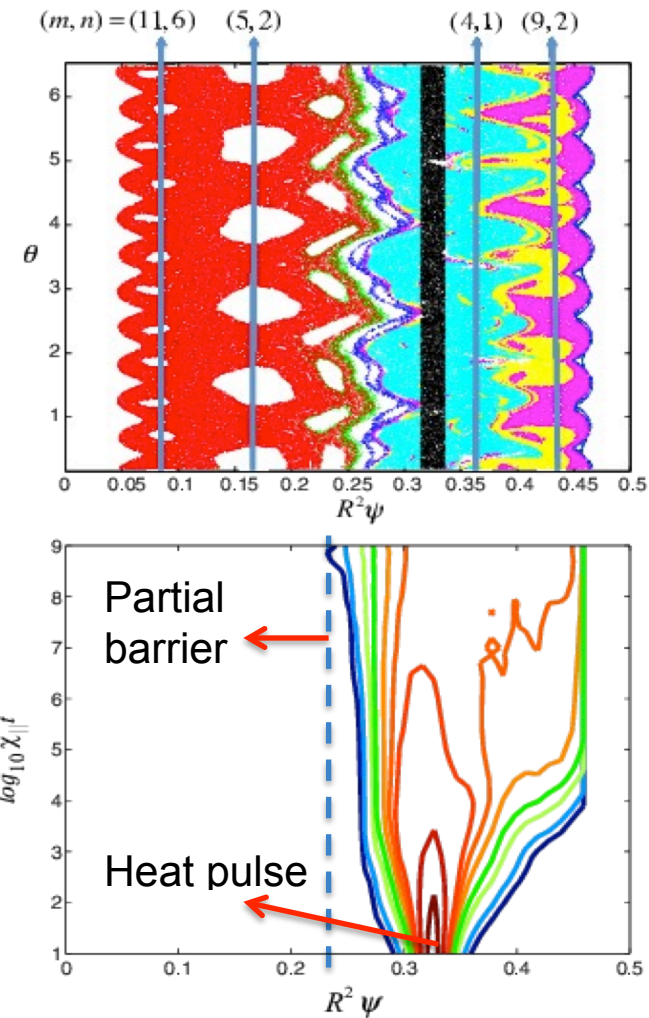


Tokamak 3D edge transport with islands, chaotic regions

- Parallel transport dominates
 - $\chi_{||}/\chi_{\perp} \sim 10^9 - 10^{10}$
- LG (Lagrangian Green's function) method
 - D. del-Castillo-Negrete, L. Chacon (2012)
 - stable, high accuracy method for high $\chi_{||}/\chi_{\perp}$ regime
 - Can treat fields with complex filamentation/braiding
 - Reduced to solution of coupled 1D ODE's
 - Transport barriers possible even with chaotic structures



Partial heat transport barriers in the absence of magnetic flux surfaces



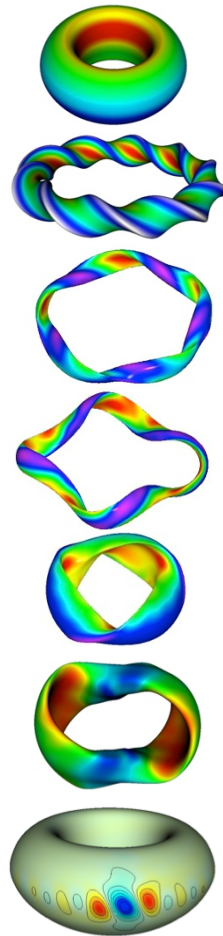
LG solution of heat transport equation in 3-D chaotic field

Stability issues for 3D configurations

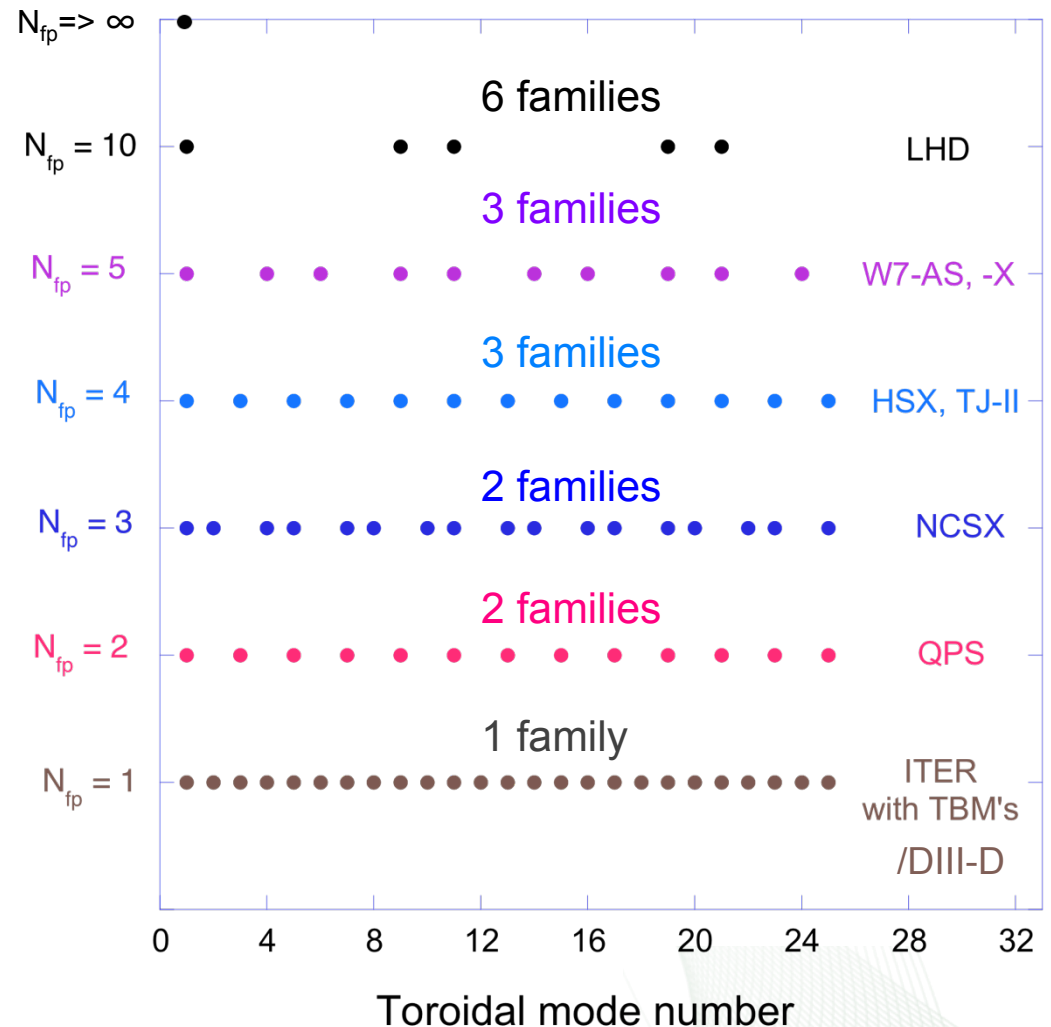
- **Energetic particle (EP) instabilities**
 - Development of EP global gyrokinetic models
 - Tokamak 3D edge effects in NSTX
- **Micro-turbulence**
 - Optimization of 3D systems for turbulent transport
- **3D tokamak edge**
 - Tearing/kink/ballooning/peeling
 - 3D perturbations can both suppress (DIII-D) and trigger (NSTX, ASDEX-upgrade) ELMs
 - Edge turbulence increase with 3D fields (G. McKee, et al., NF 2013)
 - Recent theory:
 - linear δW CAS3D stability (E. Strumberger, et al., NF, 2014)
 - 3D peeling-ballooning formulation (T. Weyens, R. Sanchez, et al., Phys. Plasmas, 2014)
- **High β stellarator regimes**
 - Soft β limit, LHD $\beta_{\text{peak}} \sim 5\%$; W7-AS $\beta_{\text{peak}} \sim 7\%$
 - Second stable hybrid systems, $\beta = 23\%$, $\beta_N = 19$ (A. Ware, PRL, 2002)

Toroidal mode number (n) is not a good quantum number for 3D configurations

- Field period symmetry: N_{fp} replicated elements
- Toroidal coupling => mode families, rather than single toroidal modes:
 $n' \pm n = kN_{fp}$, $k = 0, 1, 2, \dots$
- Finite number of families:
 $1 + N_{fp}/2$ for even N_{fp} and
 $(N_{fp}-1)/2 + 1$ for odd N_{fp}
- Computational difficulty
 - High N_{fp} easiest
 - Low N_{fp} hardest



$n = \pm 1$ mode family couplings



Gyrokinetic models for 3D configurations

- **PIC: domain divided up into cells**
 - grouped toroidally/radially for parallelization
- **Kinetic ions, fast ions: full GC orbits followed**
 - charges, currents allocated over local gyro radius template for field solve
- **Several options for electrons**
 - Adiabatic, Fluid/hybrid, Fully kinetic
- Electrostatic (ITG), electromagnetic (Alfvén instability)
- **Global vs. local**
 - GEM: flux tube approach generalized to flux surface – each field line different in 3D
 - Global: GTC, EUTERPE

Global gyrokinetic model (GTC) for Alfvén and core turbulence in 3D systems

- Global, fully electromagnetic, nonlinear kinetic-MHD processes
- Gyrokinetic ions, fluid-kinetic hybrid electrons
- General 3D (VMEC) equilibria, ported to GPU and MIC

Other GTC-related presentations:

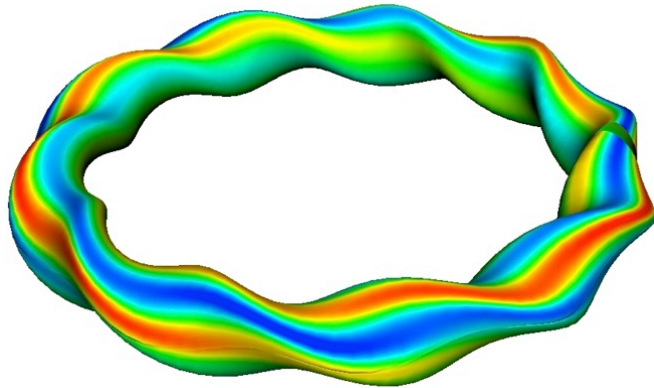
Microturbulence: JO3.00006, I. Holod; CP8.00006, Y. Xiao; CP8.00032, H. Xie; UP8.00006, D. Fulton

EP: NI1.00006, Z. Wang

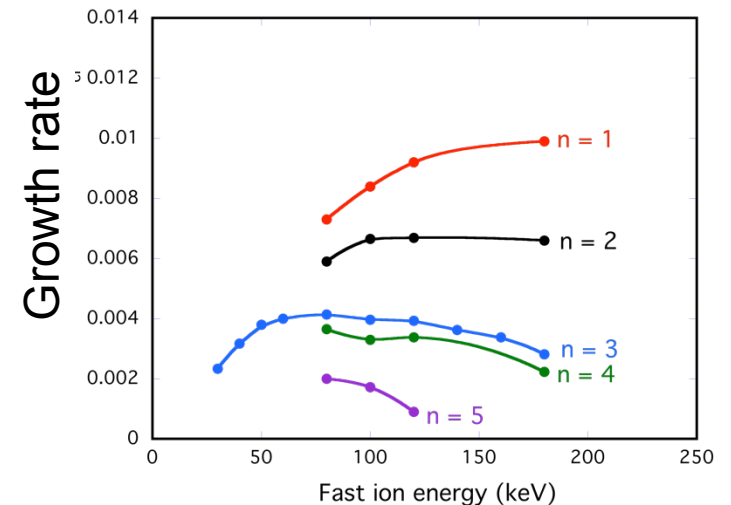
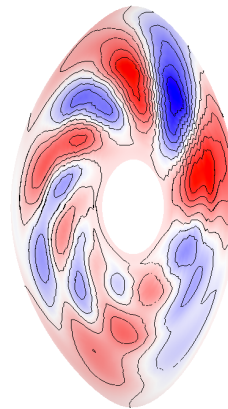
MHD: BP8.00046, D. Liu; TP8.00107, J. McClenaghan

RF: NO3.00010, J. Bao; JP8.00080 X. Wei; TP8.00055, A. Kuley

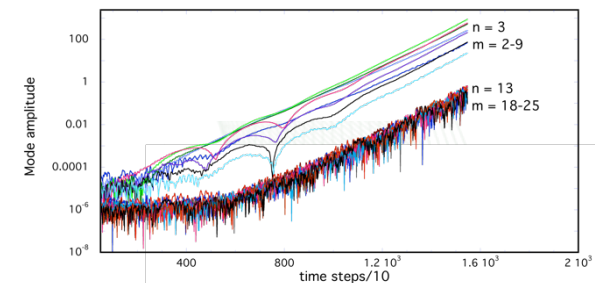
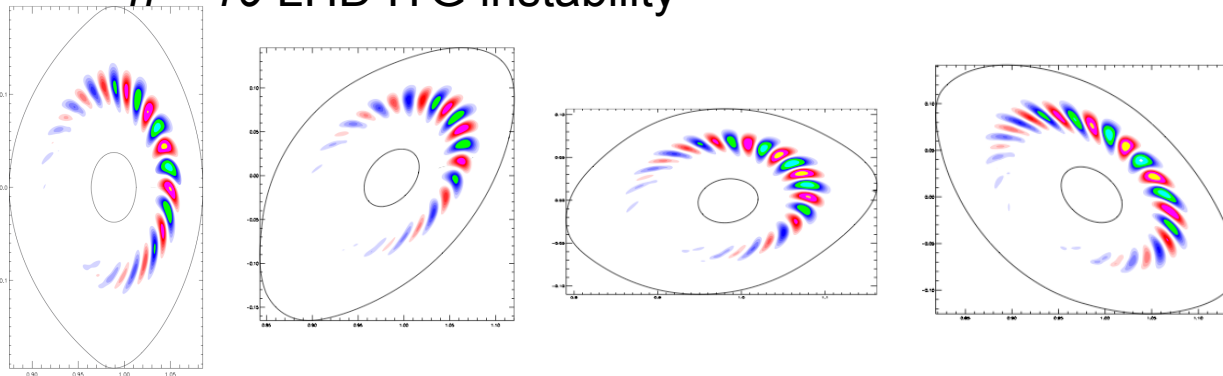
– $n = 3$ LHD Alfvén instability



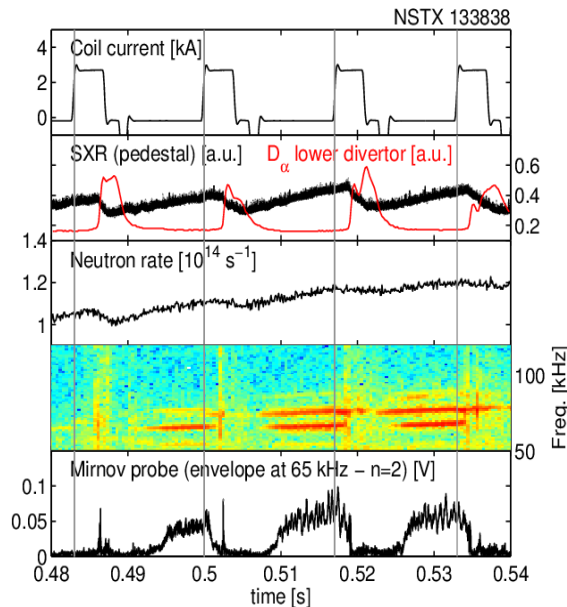
I. Holod, D. Spong, **Poster YP8.00011 APS-DPP 2014**



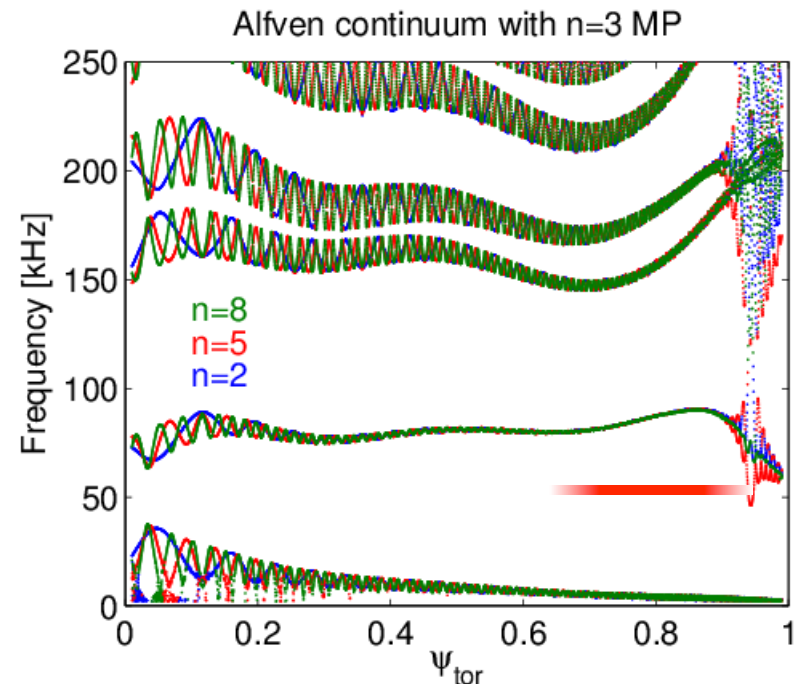
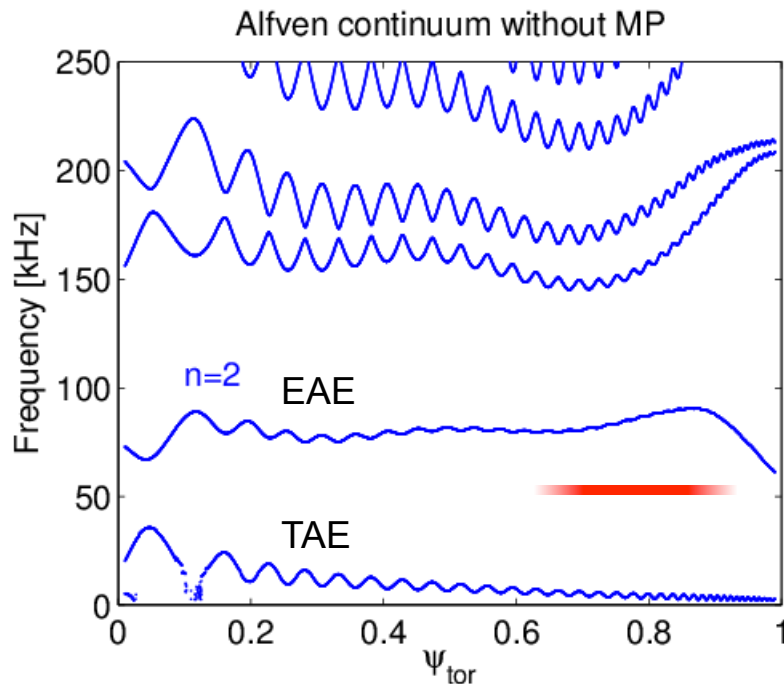
– $n = 10$ LHD ITG instability



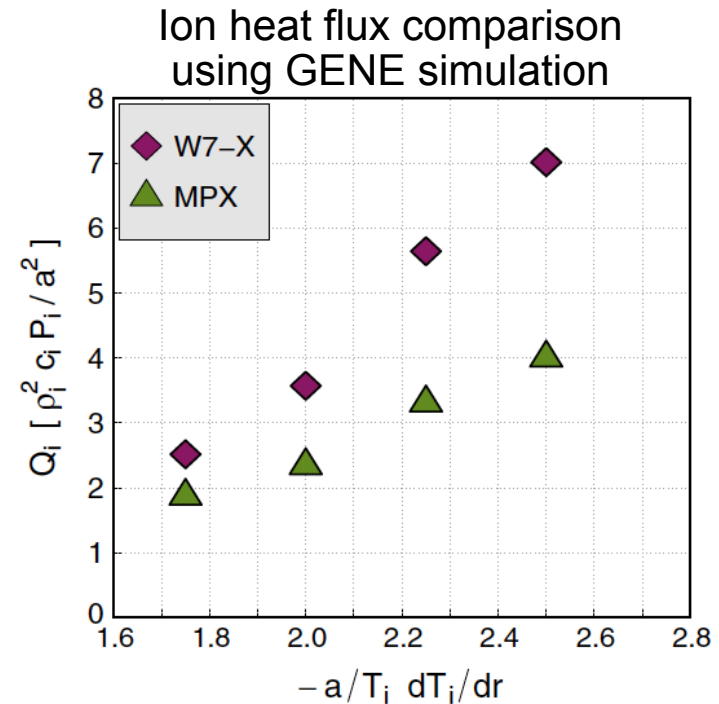
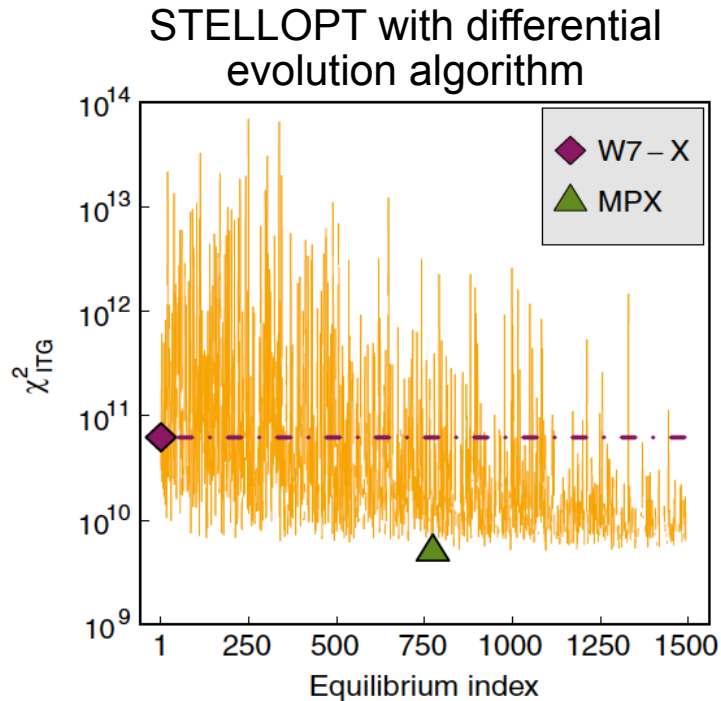
NSTX Alfvén mode suppression correlated with 3D coils



- A. Bortolon, PRL (2013), EPS (2014)
- ELMs triggered 2 ms after MP starts
- Two dominant TAEs observed
 - n=2, 65 kHz; n=3, 75 kHz
- 3D Alfvén continuum (STELLGAP model) shows toroidal coupling effects near edge => increased damping for TAE

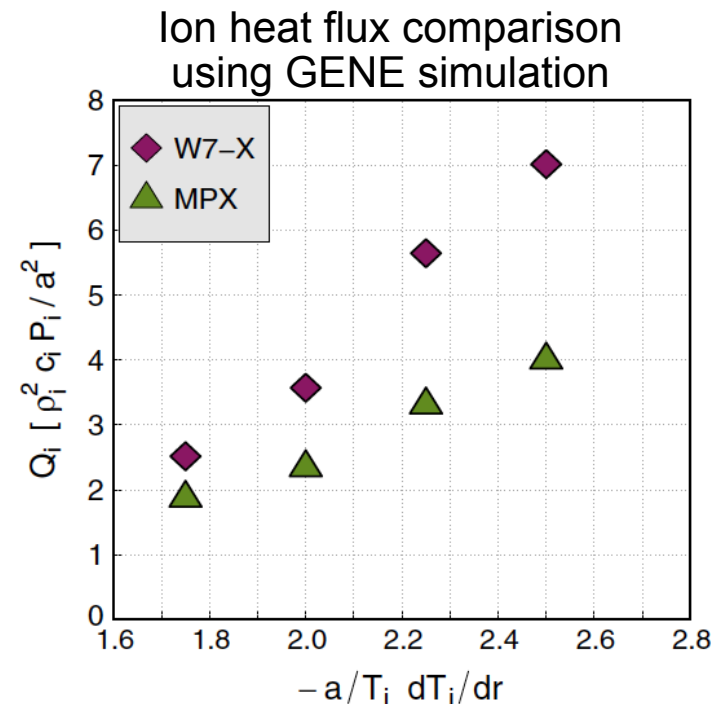
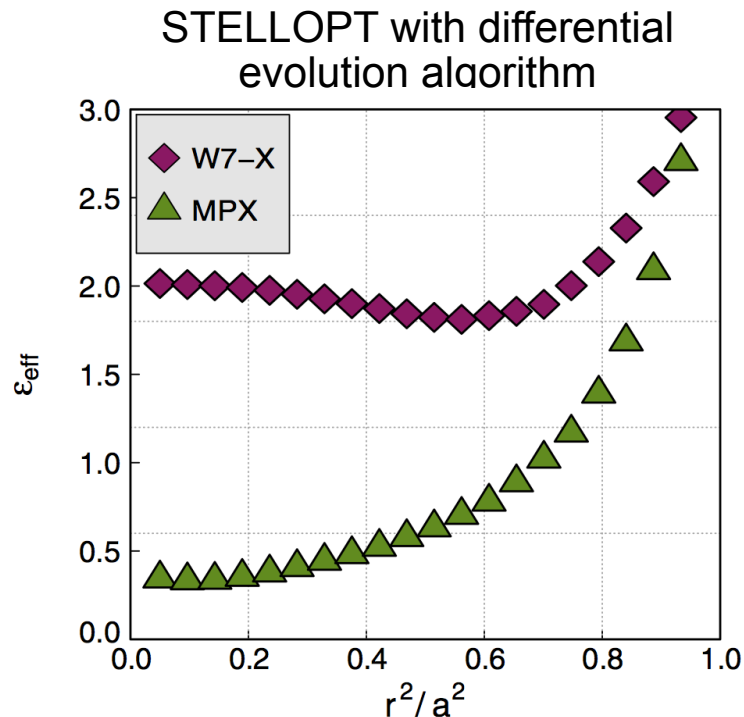


Recent GENE optimizations show that ITG turbulence is sensitive to magnetic field geometry



- GENE model: full flux surface simulation, gyrokinetic ions, Boltzmann electrons, electrostatic turbulence
- ITG optimization proxy: $\kappa_r^- (g^{rr})^2$
- P. Xanthopoulos, H. Mynick, et al., Phys. Rev. Lett. **113**, Oct. 10, 2014
- H. Mynick, P. Xanthopoulos, et al., PPCF **56** (2014)

Recent optimizations show that ITG turbulence sensitive to magnetic field geometry

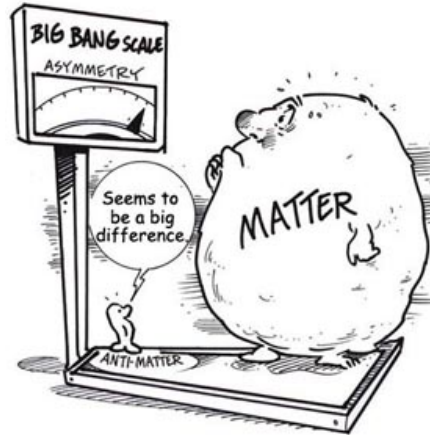
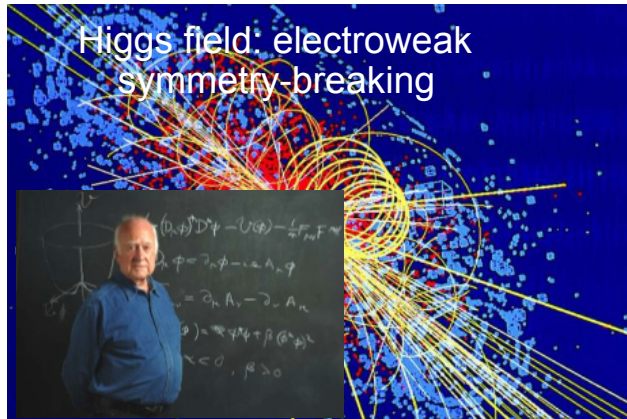


- GENE model: full flux surface simulation, gyrokinetic ions, Boltzmann electrons, electrostatic turbulence
- P. Xanthopoulos, H. Mynick, et al., Phys. Rev. Lett. **113**, Oct. 10, 2014
- J. Prohl, et al., invited talk NO3-4, this meeting, TEM stability target: minimize particles with $\omega_{*e}\omega_{de} > 0$, applied to W7-X, HSX
- G. Weir, invited talk TI1.02, this meeting, GENE application to HSX

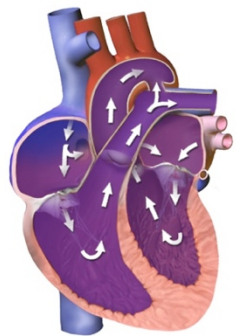
Conclusions/Summary

- **3D toroidal physics present in tokamaks/stellarators/reversed field pinches**
 - Excellent opportunity for testing/validating theory with new models applicable to all systems
- **Increasing computational resources and new theoretical methods aid in the challenge of 3D**
- **3D design/optimization: multi-physics integration, deeper design space than 2D. Opportunities:**
 - Improved RFP confinement/sustainment
 - New directions in stellarator optimization (transport, microturbulence, MHD, energetic particle physics)
 - Tokamak 3D edge (better optimization for ELM/RWM suppression, divertor structure, control of detachment and scrape-off layer)

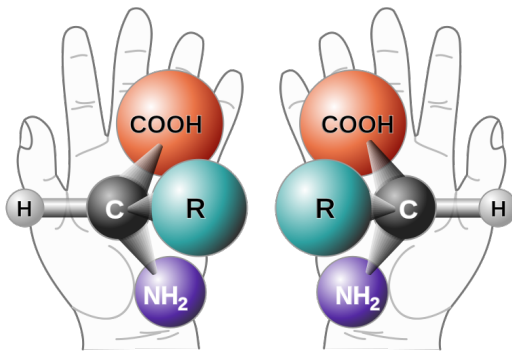
We're not alone in exploring symmetry-breaking: prevalent in nature as well as human-made objects:



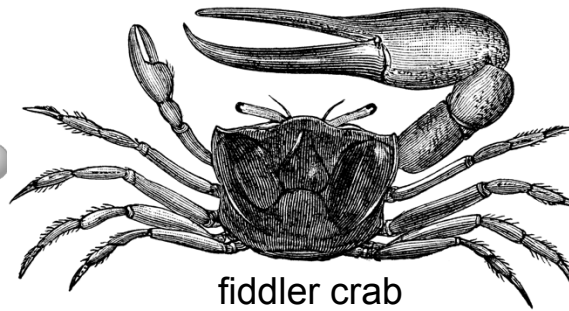
Frank Gehry architecture



Heart: left-right asymmetry



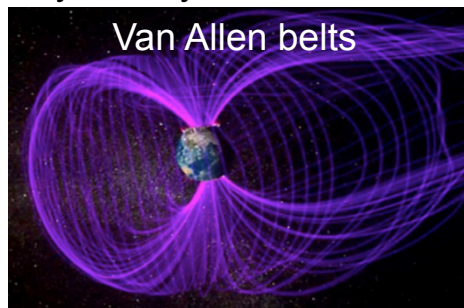
chiral amino acid molecules



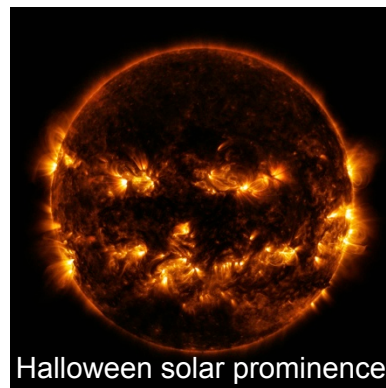
fiddler crab



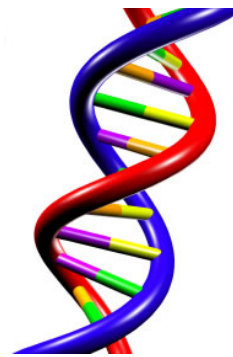
camshaft



Van Allen belts



Halloween solar prominence



DNA: right-handed helix only



Rutan asymmetric aircraft